Plant Molecular Biology (2022) 108:31–49
https://doi.org/10.1007/s11103-021-01205-0

Arabidopsis PLDζ1 and PLDζ2 localize to post-Golgi membrane compartments in a partially overlapping manner

Ryota Shimamura[1] · Yohei Ohashi[2] · Yukimi Yamamoto Taniguchi[1] · Mariko Kato[1] · Tomohiko Tsuge[1] · Takashi Aoyama[1]

Received: 17 April 2021 / Accepted: 25 September 2021 / Published online: 2 October 2021

Abstract

Key message ***Arabidopsis* PLDζ1 and PLDζ2 localize to the *trans*-Golgi network and to compartments including the *trans*-Golgi network, multi-vesicular bodies, and the tonoplast, respectively, depending on their N-terminal regions containing PX-PH domains.**

Abstract Phospholipase D (PLD) is involved in dynamic cellular processes, including membrane trafficking, cytoskeletal reorganization, and signal transduction for gene expression, through the production of phosphatidic acid in membrane compartments specific to each process. Although PLD plays crucial roles in various plant phenomena, the underlying processes involving PLD for each phenomenon remain largely elusive, partly because the subcellular localization of PLD remains obscure. In this study, we performed comparative subcellular localization analyses of the *Arabidopsis thaliana* PX-PH-PLDs PLDζ1 and PLDζ2. In mature lateral root cap cells, own promoter-driven fluorescence protein fusions of PLDζ1 localized to the entire *trans*-Golgi network (TGN) while that of PLDζ2 localized to punctate structures including part of the TGN and multi-vesicular bodies as well as the tonoplast. These localization patterns were reproduced using N-terminal partial proteins, which contain PX-PH domains. An inducibly overexpressed fluorescence protein fusion of the PLDζ2 partial protein first localized to punctate structures, and then accumulated predominantly on the tonoplast. Further domain dissection analysis revealed that the N-terminal moiety preceding the PX-PH domain of PLDζ2 was required for the tonoplast-predominant accumulation. These findings suggest that PLDζ1 and PLDζ2 play partially overlapping but nonetheless distinctive roles in post-Golgi compartments along the membrane trafficking pathway from the TGN to the tonoplast.

Keywords *Arabidopsis thaliana* · Phospholipase D · *Trans*-Golgi network · Multivesicular body · Tonoplast · PX-PH domain

✉ Takashi Aoyama
aoyama@scl.kyoto-u.ac.jp

Ryota Shimamura
shimamura.ryota.6j@kyoto-u.ac.jp

Yohei Ohashi
yo@mrc-lmb.cam.ac.uk

Yukimi Yamamoto Taniguchi
blessing0521@gmail.com

Mariko Kato
kato@scl.kyoto-u.ac.jp

Tomohiko Tsuge
tsuge@scl.kyoto-u.ac.jp

[1] Institute for Chemical Research, Kyoto University, Gokasho, Uji, Kyoto 611-0011, Japan

[2] MRC Laboratory of Molecular Biology, University of Cambridge, Francis Crick Avenue, Cambridge Biomedical Campus, Cambridge CB2 0QH, UK

Introduction

Phospholipases are a group of enzymes hydrolyzing phospholipids, ubiquitous membrane lipids in living organisms, and are classified into several types by specificities of their enzymatic activities (Filkin et al. 2020). Phospholipase A_1 (PLA_1) and phospholipase A_2 (PLA_2) cleave the *sn*-1 and *sn*-2 positions of the acyl group, respectively, to produce a free fatty acid and a lysophospholipid (Chen et al. 2013). Phospholipase C (PLC) and phospholipase D (PLD) produces diacylglycerol (DAG) and phosphatidic acid (PA), respectively, by hydrolyzing the phosphodiester bond between the glycerol backbone and a head group (Frohman and Morris 1999; Liscovitch et al. 2000; Munnik 2014; Nakamura 2014).

Among them, PLD is involved in dynamic cellular processes, including membrane traffic, cytoskeletal reorganization, and signal transduction for gene expression, via PA production in membrane compartments specific to each process (Jenkins and Frohman 2005; Roth 2008; Pleskot et al. 2013; Zhukovsky et al. 2019). PA functions as a second messenger to recruit various regulatory proteins or modulate their activities spatiotemporally (Stace and Ktistakis 2006). The unbalanced cross-section caused by the polar head and hydrophobic chain moieties of PA facilitates local membrane curvature for dynamic membrane deformation processes such as membrane fission and fusion (Kooijman et al. 2003; McMahon and Gallop 2005; Donaldson 2009). Moreover, PA serves as a substrate for the production of other membrane lipids, such as diacylglycerol and diacylglycerol pyrophosphate, which have different molecular functions from PA (Athenstaedt and Daum 1999; Munnik 2001). This multi-functionality of PA hampers the elucidation of the mechanisms through which PLD is involved in dynamic cellular processes.

In higher plants, PLD plays crucial roles in physiological phenomena during development and in response to environmental stimuli (Testerink and Munnik 2011; Kolesnikov et al. 2012; Hong et al. 2016). Plant PLDs are classified based on their structure into two subfamilies: plant-specific C2-PLDs (α-, β-, γ-, δ-, and ε-type PLDs), which contain the calcium-dependent phospholipid-binding (C2) domain, and PX-PH-PLDs (ζ-type PLDs), which are common to eukaryotes and contain the phox and pleckstrin homology (PX-PH) domain (Eliáš et al. 2002; Qin and Wang 2002). Genetic studies of *Arabidopsis thaliana* have demonstrated the involvement of PLDs in environmental responses (Li et al. 2009; Kolesnikov et al. 2012). However, no single mutant exhibits developmental phenotypes under normal growth conditions, possibly due to functional compensation by other PLDs or other lipid-metabolizing enzymes (Munnik 2001; Raghu et al. 2009; Bankaitis 2012).

Arabidopsis C2-PLD genes have been reported to function in environmental responses (Li et al. 2009; Kolesnikov et al. 2012). *pldα1*, *pldα3*, *pldδ*, and *pldε* mutants are hypersensitive to salt and osmotic stresses (Hong et al. 2008, 2009; Bargmann et al. 2009). The *pldδ* mutant is also hypersensitive to H_2O_2 and freezing stresses (Zhang et al. 2003; Li et al. 2004), but is hyposensitive to severe drought stress (Distéfano et al. 2015). The responses to nitrogen deprivation and aluminum stress are altered in *pldε* and *pldγ1* mutants, respectively (Hong et al. 2009; Zhao et al. 2011). For biotic stressors, the growth promotion in response to the beneficial fungus *Piriformospora indica* is impaired in *pldα1* and *pldδ* mutants (Camehl et al. 2011). Penetration resistance against non-host powdery mildew fungi is also impaired in the *pldδ* mutant (Pinosa et al. 2013; Johansson et al. 2014). *pldβ1* mutant plants are hypersensitive to the necrotrophic pathogen *Botrytis cinerea*, but are hyposensitive to the biotrophic pathogen *Pseudomonas syringae* pv. tomato DC3000 (Zhao et al. 2013), whereas *pldγ1* mutant plants are hyposensitive to both pathogens (Schlöffel et al. 2020).

Although various PA-interacting proteins have been suggested to function in these environmental responses (Mcloughlin and Testerink 2013; Yao and Xue 2018; Pokotylo et al. 2018; Li and Wang 2019), the downstream molecular mechanisms of particular PLDs have rarely been clarified. During ABA-mediated stomatal closure, PLDα1-produced PA tethers the PP2C-type protein phosphatase ABI1 to the plasma membrane and prevents its suppression of ABA signaling to support gene expression in the nucleus (Zhao and Wang 2004; Zhang et al. 2004; Mishra et al. 2006). Concurrently, PA binds to NADPH oxidases on the plasma membrane to stimulate the production of H_2O_2, which oxidizes intracellular factors including cytosolic glyceraldehyde-3-phosphate dehydrogenases (Zhang et al. 2009; Guo et al. 2012). In response to high salinity, PLDα1-produced PA directly activates the mitogen-activated protein kinase MPK6 to phosphorylate the plasma membrane Na^+/H^+ antiporter SOS1 (Yu et al. 2010) and the microtubule-associated protein MAP65-1 (Zhang et al. 2012). During *P. indica* infection, PA produced by PLDα1 or PLDδ directly activates PDK1s, homologs of 3-phosphoinositide-dependent protein kinase 1, which then activate OXI1, a protein kinase involved in pathogen responses (Camehl et al. 2011).

The *Arabidopsis* PX-PH-PLD genes *PLDζ1* and *PLDζ2* are involved in both developmental processes and environmental responses (Li et al. 2009; Kolesnikov et al. 2012). The *PLDζ1* gene is repressed directly by the transcription factor GL2 in non-root hair cells during root hair development, and its suppression with inducible anti-sense RNA results in abnormal root hair morphologies (Ohashi et al. 2003). A genetic study employing a PX-PH-PLD-specific inhibitor indicated that PLDζ1 plays a role in the negative feedback regulation of root hair development in non-root hair cells (Yao et al. 2013). Under phosphate deprivation conditions, *PLDζ1* and *PLDζ2* are transcriptionally activated and play roles in altering membrane lipid composition from phospholipids to galactolipids to support phosphate recycling (Cruz-Ramírez et al. 2006; Li et al. 2006a, 2006b; Su et al. 2018). Phosphate deprivation impairs the growth and apical meristem organization of primary roots more severely in *pldζ2* mutant plants than in wild-type plants (Cruz-Ramirez et al. 2006; Su et al. 2018). Recently, PLDζ2 has been suggested to suppress vacuolar accumulation of the auxin efflux transporter PIN2 and support enhanced root hair elongation under phosphate deprivation conditions (Lin et al. 2020). *pldζ2* mutants exhibited reduced root tropism, including gravitropism, hydrotropism, and halotropism (Li and Xue 2007; Taniguchi et al. 2010; Galvan-Ampudia et al.

2013). The *pldζ2* mutation has been shown to affect endocytosis and vesicle trafficking, impacting PIN2 relocalization in root epidermal cells during auxin-related phenomena, including root tropic responses (Li and Xue 2007; Galvan-Ampudia et al. 2013). Gravitropic and halotropic responses are affected also in the mutant roots of the *PLDζ1* gene, which is involved in dynamic PIN2 localization patterns in root epidermal cells (Korver et al. 2019).

Several molecular mechanisms have been proposed for functions of PA produced by PLDζ1 or PLDζ2. In the negative feedback regulation of root hair development, PLDζ1-produced PA is assumed to bind to the transcription factor WER to assist in its nuclear translocation (Yao et al. 2013). PLDζ2-produced PA is assumed to bind to the protein phosphatase PP2A, which dephosphorylates PINs to modulate their subcellular localization (Michniewicz et al. 2007; Gao et al. 2013), and to the endosomal regulatory protein SNX1, which is involved in vacuolar sorting of PIN2 (Kleine-Vehn et al. 2008; Lin et al. 2020). However, the molecular mechanisms of these processes have not been fully elucidated, as subcellular localizations of PLDζ1 and PLDζ2 responsible for the PA production remain unclear. Although PLDζ1-GFP driven by its own promoter localizes to the cell cortical region and vesicular structures in root hair cells (Ohashi et al. 2003), the compartments that contribute to this pattern and whether the pattern is common among cell types are unknown. PLDζ2-GFP ectopically overexpressed by the cauliflower mosaic virus 35S promoter has been reported to localize to the tonoplast in leaf epidermal cells of pea and *Arabidopsis* plants (Yamaryo et al. 2008). However, how accurately this localization pattern reflects the endogenous pattern remains unknown.

In this study, we performed comparative subcellular localization analyses of PLDζ1 and PLDζ2 for a clue about mechanisms of their roles in physiological phenomena. Our results indicated that PLDζ1 and PLDζ2 localize to the *trans*-Golgi network (TGN) and to membrane compartments along a post-Golgi trafficking pathway to the tonoplast, respectively, depending on their N-terminal regions containing PX-PH domains, suggesting that they play partially overlapping but nonetheless distinctive roles in these post-Golgi membrane compartments.

Materials and methods

Plant material and growth conditions

Arabidopsis thaliana ecotype Columbia-0 was used as the wild type. The T-DNA insertion line *pldζ2* (SALK_094369) was obtained from the Arabidopsis Biological Resource Center (Alonso et al. 2003). Seeds were surface-sterilized and germinated on vertically standing Murashige-Skoog (MS) agar plates containing MS salts (Murashige and Skoog 1962), B5 vitamins, 2.3 mM MES-KOH (pH 5.7–5.8), 1% (w/v) sucrose, and 1.6% agar. Seedlings were grown at 22 °C under continuous light conditions unless otherwise noted.

Construction of transgenes and transgenic lines

Previously reported 1079-bp and 1408-bp upstream intergenic regions (Ohashi et al. 2003; Taniguchi et al. 2010) were used as the *PLDζ1* and *PLDζ2* promoter fragments, respectively. The transgene *PLDζ1p-PLDζ1-mCherry* was constructed with the *PLDζ1* promoter fragment and that containing the coding sequence of PLDζ1 cDNA followed in-frame by the mCherry-coding sequence (Clontech, Mountain View, CA, USA) in the binary vector pHPT121 (Kusano et al. 2008). The transgene *PLDζ2p-PLDζ2-GFP* was constructed with the *PLDζ2* promoter fragment and that containing the coding sequence of PLDζ2 cDNA, followed in-frame by the GFP-coding sequence (Chiu et al. 1996) in the binary vector pHPT121. The transgenes *PLDζ1p-NPXPH1-mCitrine* and *PLDζ2p-NPXPH2-tdTomato* were constructed with the *PLDζ1* and *PLDζ2* promoter fragments, and the coding fragments of the 340-amino-acid N-terminal region of PLDζ1, NPXPH1, fused to mCitrine (Griesbeck et al. 2001) and the 341-amino-acid N-terminal region of PLDζ2, NPXPH2, fused to tdTomato (Invitrogen, Carlsbad, CA, USA), respectively, in pHPT121. The coding fragments of NPXPH1 and NPXPH2 fused to mCitrine and mCherry were placed downstream of the 35S promoter in pHPT121 for overexpression, and the β-estradiol-inducible promoter in pER8 (Zuo et al. 2000) for inducible expression. For functional dissection of NPXPH1 and NPXPH2, fragments coding their chimeric and truncated proteins fused to mCitrine were placed downstream of the 35S promoter in pHPT121. The transgene expressing tdTomato by the *BFN1* promoter was constructed with the 668-bp genomic fragment immediately preceding the *BFN1* initiation codon (Fendrych et al. 2014) and the tdTomato-coding sequence in pBAR121, a binary vector in which the kanamycin resistance gene of pBI121 (Clontech) was replaced with a Basta resistance gene (Thompson et al. 1987). Transgenes constructed in this study, including those of marker genes, are listed in Supplementary Table S1. Junction sequences in the transgene constructs are described in Supplementary Table S2. Transgenic *Arabidopsis* lines were made using the *Agrobacterium tumefaciens*-mediated floral dip method (Clough and Bent 1998). For each transgenes, more than 10 independent transgenic lines were obtained, and consistent experimental results were confirmed in at least 4 lines. Of those, one or two representative lines were crossed with other transgenic lines in the case of their co-expression. The transgenic line harboring the *pPLDζ1::PLDζ1-YFP* gene was described previously (Korver et al. 2019).

Confocal laser scanning microscopy

Roots of seedlings grown on vertical MS agar plates for 5 days after germination were subjected to the observation of fluorescence protein fusions unless otherwise noted. Fluorescence images were captured using a microscope (Axio Observer Z1, Carl Zeiss, Oberkochen, Germany) equipped with a confocal laser-scanning unit (CSU-X1, Yokogawa, Tokyo, Japan). Excitation beams of 488 nm for GFP, mGFP, YFP, and mCitrine, and 561 nm for mCherry, mRFP, tdTomato, and FM4-46 were used. Detection bands of 499–529 nm for GFP and mGFP, 515–543 nm for mCitrine and YFP, and 612–638 nm for mCherry, mRFP, tdTomato, and FM4-46 were used.

Quantitative co-localization analyses of fluorescence signals

For coincidence of punctate structures detected by different fluorescences, more than 100 punctate signals for each fluorescence protein fusion were selected from pairs of different fluorescence images using the Find Maxima process in the ImageJ software with appropriate Prominence values for each fusion protein. For each selected signal on one fluorescence image, the distance from its center to that of the closest signal on the other fluorescence image was calculated. Then, the signals with the distance no more than 0.42 µm, more than 0.42 µm and no more than 1.69 µm, and more than 1.69 µm were counted. The ratio of the signals with the distance no more than 0.42 µm was statistically estimated for each pair of fluorescence protein fusions. For co-localization of fluorescence protein fusions of chimeric and truncated constructs, values of the linear Pearson correlation coefficient (r_p) and the non-linear Spearman's rank (r_s) were calculated between each pair of different fluorescence images using the Coloc2 analysis in the ImageJ software with PSF and Costes randomisations parameter values of 3.0 and 10, respectively.

Chemical treatments

Brefeldin A (BFA) and wortmannin (Wm) treatments were performed by transferring seedlings grown on vertical MS agar plates for 7 days after germination into MS liquid medium containing 50 µM BFA [stock solution: 50 mM BFA in dimethyl sulfoxide (DMSO)] for 20 min and that containing 33 µM Wm (stock solution: 33 mM Wm in DMSO) for 1 h, respectively. For inducible expression, seedlings grown on vertical MS agar plates for 7 days after germination were transferred into MS liquid medium containing 30 µM β-estradiol (stock solution: 100 mM stock β-estradiol in DMSO) and observed after appropriate time periods. For staining with FM4-64, roots were treated with MS liquid medium containing 2 µM FM4-64 (stock solution: 2 mM FM4-64 in DMSO) for 5 min before observation.

Analysis of root gravitropic responses

Seedlings of the wild type, *pldζ2* mutants, and the transformation rescue line *PLDζ2p-PLDζ2-GFP/pldζ2* were germinated on vertical MS agar plates. At 5 days after germination, plates containing seedlings were rotated 90°, and root images were captured after 0 and 5 h. Changes in the root growth direction from that at 0 h were measured each seedling on images using the ImageJ software.

Quantitative real-time RT-PCR

Total RNA was isolated from seedlings using ISOGEN (Nippon Gene, Tokyo, Japan) according to the manufacturer's protocol. For reverse transcription, first-strand cDNA was synthesized from total RNA using ReverTra Ace® qPCR RT Master Mix with gDNA Remover (TOYOBO, Osaka, Japan). The cDNA was used in quantitative real-time PCR with THUNDERBIRD SYBR qPCR Mix (TOYOBO). The relative transcript level was determined using the delta-delta-Ct method. The primer sets used for real-time PCR are listed in Supplementary Table S3.

Results

Own promoter-driven fluorescence protein fusions of PLDζ1 and PLDζ2 were detected in various types and one specific type of root cells, respectively

To analyze the subcellular localization of PLDζ1 and PLDζ2 in cells under endogenous expression conditions, we constructed the reporter genes *PLDζ1p-PLDζ1-mCherry* and *PLDζ2p-PLDζ2-GFP*, in which sequences encoding fluorescence protein fusions of PLDζ1 and PLDζ2 were paired with upstream intergenic sequences of the *PLDζ1* and *PLDζ2* genes, respectively, and introduced these constructs into the wild-type *Arabidopsis*. We also used the reporter gene *pPLDζ1::PLDζ1-YFP*, which has the same structure as *PLDζ1p-PLDζ1-mCherry* except for the fused fluorescence protein and has been reported to rescue the *pldζ1* phenotype of exaggerated root gravitropism (Korver et al. 2019). To examine the functionality of *PLDζ2p-PLDζ2-GFP*, we introduced the transgene into a *pldζ2* mutant through crossing of the established transgenic line with the mutant, and confirmed that it rescued the *pldζ2* phenotype of retarded root gravitropism (Li and Xue 2007) (Supplementary Fig. S1).

We first observed cell type-specific expression patterns of these reporter genes on the root surface, where highly

sensitive detection of fluorescence proteins via confocal laser scanning microscopy is feasible. Consistent with a previous result of the β-glucuronidase (GUS) reporter analysis (Ohashi et al. 2003), fluorescence of PLDζ1-mCherry and PLDζ1-YFP was observed in root epidermal cells, including root hair cells (Supplementary Figs. S2a, b, S3). Columella and lateral root cap cells, and root cortex cells also expressed these genes (Fig. 1a, b and Supplementary Figs. S2a, b, S3, S4). Fluorescence of PLDζ2-GFP was clearly observed in mature lateral root cap cells (Fig. 1a, b and Supplementary Fig. S2c) as previously shown in the GUS reporter analysis (Cruz-Ramírez et al. 2006; Li and Xue 2007; Taniguchi et al. 2010). However, no fluorescence was detectable in columella root cap cells, root cortex cells, or root epidermal cells including root hair cells and those beneath lateral root cap cells (Fig. 1a and Supplementary Figs. S2c, S4, S5a); faint signals observed in these cells are thought to be due to plant autofluorescence, as similar signals were observed in wild-type and *PLDζ1p-PLDζ1-mCherry* roots using the same microscopic settings for GFP detection (Fig. 1a and Supplementary Figs. S2d, S4, S5a). In transgenic plants harboring *PLDζ2p-PLDζ2-GFP* and a *BFN1* promoter-driven tdTomato gene, the expression of which precedes developmental programmed cell death in lateral root cap cells (Fendrych et al. 2014), the cell types expressing tdTomato included those expressing PLDζ2-GFP (Supplementary Fig. S5b), indicating that PLDζ2-GFP was expressed specifically in lateral root cap cells during the stage preceding developmental programmed cell death.

Own promoter-driven fluorescence protein fusions of PLDζ1 localized throughout the TGN marked by SYP43

To comparatively analyze the subcellular localization patterns of PLDζ1 and PLDζ2, we observed mature lateral root cap cells, in which fluorescence protein fusions of both PLDζ1 and PLDζ2 were detectable. In these cells, the fluorescence signals of PLDζ1-mCherry and PLDζ1-YFP were localized to punctate structures (Figs. 1c and 2a), as previously observed in root hairs (Ohashi et al. 2003), and overlapped exactly in cells expressing both fusion proteins (Fig. 2a). Dispersed fluorescence was also detected in the cytoplasmic space (Fig. 1c). To identify the compartments corresponding to the observed punctate structures, we co-expressed a series of membrane compartment markers, including GFP-SYP32 for the Golgi (Uemura et al. 2004; Geldner et al. 2009), ST-mGFP for *medial*- and *trans*-Golgi (Boevink et al. 1998), GFP-SYP43 and mRFP-SYP43 for the entire TGN including Golgi-associated (GA-) and Golgi-released independent (GI-) TGNs (Uemura et al. 2012, 2014, 2019), GFP-VAMP721 for compartments associated with the secretory pathway-associated GI-TGN (Uemura et al. 2019), and GFP-ARA7 for compartments associated with multi-vesicular bodies (MVBs) (Ueda et al. 2001; Kotzer et al. 2004; Lee et al. 2004).

Among these markers, PLDζ1-mCherry and PLDζ1-YFP were strongly co-localized with GFP-SYP43 and mRFP-SYP43, respectively, in the punctate structures (Fig. 2d, e). The locations of punctate signals for PLDζ1-mCherry and PLDζ1-YFP appeared to coincide almost completely with the GFP-SYP43 and mRFP-SYP43 signals, respectively, and values of their coincidence were almost equal to those of the positive control pair mRFP-SYP43 and GFP-SYP43 (Fig. 2l, m, p, Supplementary Fig. S6a, b). In addition, coincidence values of PLDζ1-mCherry were higher with GFP-VAMP721 than with GFP-SYP32, ST-mGFP, or GFP-ARA7 (Fig. 2j, k, n, o and Supplementary Fig. S6a, b), and higher with ST-mGFP than with GFP-SYP32 (Fig. 2j, k and Supplementary Fig. S6a, b). These results indicate that fluorescence protein fusions of PLDζ1 localize strongly to the entire TGN, including the GA-TGN and GI-TGN. Supporting this, treatment with BFA, which aggregates the TGN in large endomembrane compartments called BFA bodies that are surrounded by the Golgi apparatus (Geldner et al. 2009), caused PLDζ1-mCherry to co-localize with GFP-SYP43 in large punctate structures surrounded by ST-mGFP (Fig. 2q, r). In root epidermal meristematic cells, PLDζ1-mCherry exhibited nearly identical co-localization patterns with the markers to those in mature lateral root cap cells (Supplementary Figs. S6e, f, S7). GFP-SYP43 and GFP-VAMP721, but not PLDζ1-mCherry, were also present on the plasma membrane of root epidermal meristematic cells as observed in previous studies (Uemura et al. 2012; Zhang et al. 2015), presumably reflecting the fact that functions of both SYP43 and VAMP72 are closely related to membrane traffic to the plasma membrane (Uemera et al. 2019).

Own promoter-driven fluorescence protein fusion of PLDζ2 localized to the tonoplast and ARA7-marked membrane compartments including MVBs

Ectopically overexpressed PLDζ2-GFP has been shown to localize predominantly to the tonoplast in leaf epidermal cells (Yamaryo et al. 2008). However, PLDζ2-GFP expressed under the *PLDζ2* promoter exhibited punctate and dispersed signals in the cytoplasmic space as well as on the tonoplast in mature lateral root cap cells (Fig. 1c). In cells expressing both PLDζ1-mCherry and PLDζ2-GFP, the two signals partially co-localized on punctate structures (Fig. 1c, d and Supplementary Fig. S6a, c). To identify the compartments harboring PLDζ2-GFP, fluorescence marker proteins including mRFP-SYP43 for the entire TGN, mRFP-ARA7 for compartments associated with MVBs, and 2xmCherry-ATG8a for autophagosomes (Yoshimoto et al.

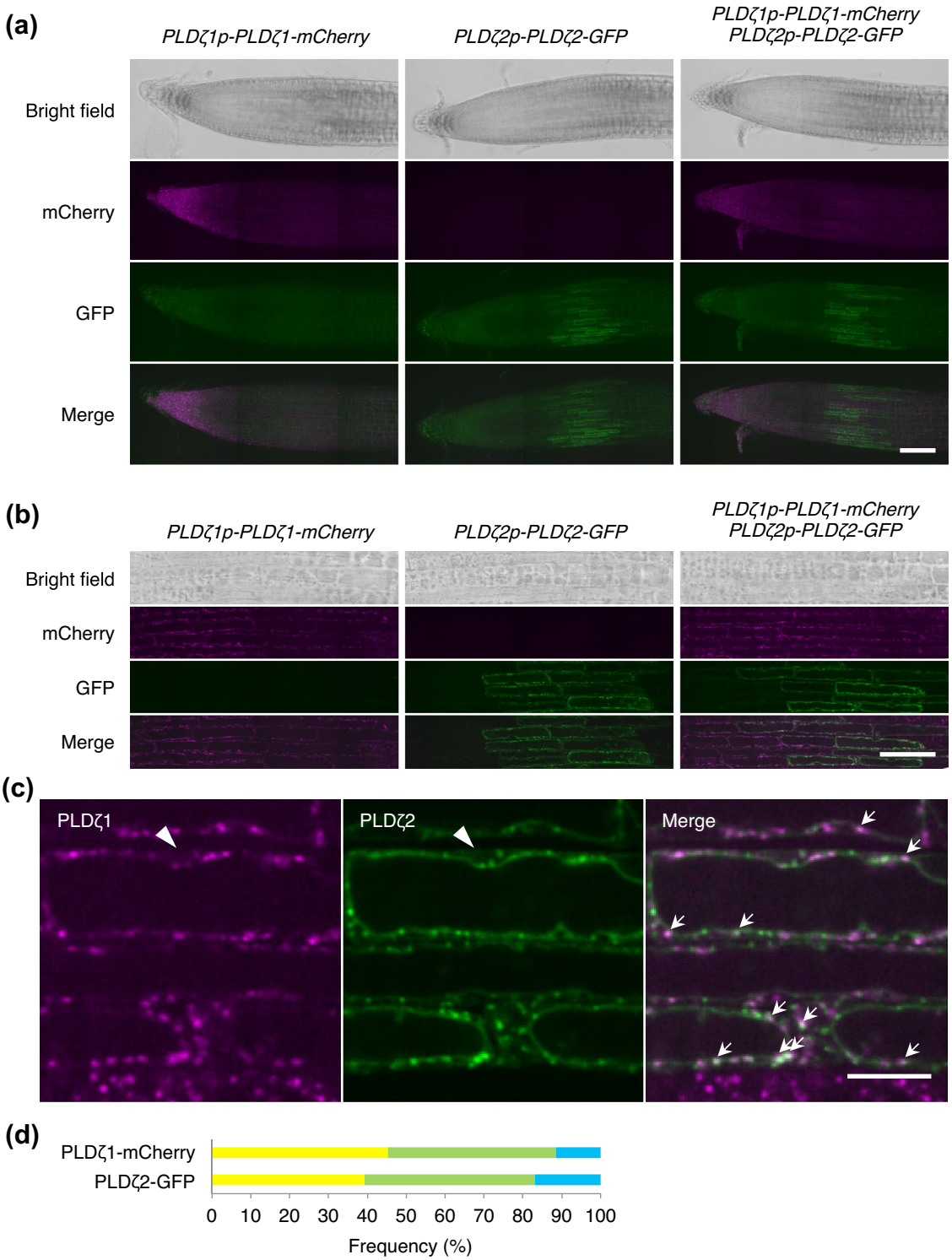
(a)
PLDζ1p-PLDζ1-mCherry
PLDζ2p-PLDζ2-GFP
PLDζ1p-PLDζ1-mCherry
PLDζ2p-PLDζ2-GFP
Bright field
mCherry
GFP
Merge
(b)
PLDζ1p-PLDζ1-mCherry
PLDζ2p-PLDζ2-GFP
PLDζ1p-PLDζ1-mCherry
PLDζ2p-PLDζ2-GFP
Bright field
mCherry
GFP
Merge
(c)
PLDζ1
PLDζ2
Merge
(d)
PLDζ1-mCherry
PLDζ2-GFP
0 10 20 30 40 50 60 70 80 90 100
Frequency (%)

◂**Fig. 1** Expression analyses of *PLDζ1p-PLDζ1-mCherry* and *PLDζ2p-PLDζ2-GFP* in the root tip region. **a**, **b** Transgenic seedlings harboring *PLDζ1p-PLDζ1-mCherry*, *PLDζ2p-PLDζ2-GFP*, or both were observed to determine the expression patterns of PLDζ1-mCherry and PLDζ2-GFP in the root tip region (**a**) and on the lateral root cap surface (**b**). Bright-field images and mCherry, GFP, and merged fluorescence images are shown. The left side of each image corresponds to the root apical side. Fluorescence in *PLDζ1p-PLDζ1-mCherry* roots and *PLDζ2p-PLDζ2-GFP* roots observed under the same microscopic settings as those for GFP fluorescence in *PLDζ2p-PLDζ2-GFP* roots and mCherry fluorescence in *PLDζ1p-PLDζ1-mCherry* roots, respectively, are shown as references for plant autofluorescence. **c** Mature lateral root cap cells harboring both *PLDζ1p-PLDζ1-mCherry* and *PLDζ2p-PLDζ2-GFP* were observed to compare the subcellular localization patterns of PLDζ1-mCherry and PLDζ2-GFP. The mCherry, GFP, and merged fluorescence images are shown. Arrowheads in the mCherry and GFP images indicate dispersed fluorescence signals in the cytoplasmic space. Arrows in the merged image indicate typical punctate structures containing both mCherry and GFP fluorescence signals. **d** The result of quantitative coincidence analysis of punctate structures containing mCherry and GFP signals is shown. For each punctate signal of mCherry or GFP fluorescence in cells obviously expressing both PLDζ1-mCherry and PLDζ2-GFP, the distance from its center to that of the closest signal of the other fluorescence was calculated. Punctate signals with the distance no more than 0.42 µm (yellow), more than 0.42 µm and no more than 1.69 µm (green), and more than 1.69 µm (blue) were counted, and their ratios are shown in a stacked bar graph for each fluorescence protein. The % values (mean ± SD, $n = 3$) of coincident puncta with the distance no more than 0.42 µm and results of statistical analysis are shown in Supplemental Fig. S6a and c. Bars = 100 µm (**a**), 50 µm (**b**), 10 µm (**c**)

2004) were co-expressed, along with the tonoplast marker VHP1-mCherry (Segami et al. 2014).

Among these markers, mRFP-ARA7 closely co-localized with PLDζ2-GFP on punctate structures (Fig. 3b). The coincidence values between PLDζ2-GFP and mRFP-ARA7 were comparable to those of the positive control pair GFP-ARA7 and mRFP-ARA7 (Fig. 3g, i and Supplementary Fig. S6c, d), indicating that the punctate structures harboring PLDζ2-GFP basically coincide with those harboring mRFP-ARA7. Consistent with the almost complete and partial co-localization patterns of PLDζ1-mCherry with GFP-SYP43 and PLDζ2-GFP, respectively (Figs. 1c and 2d), PLDζ2-GFP co-localized partially with mRFP-SYP43 (Fig. 3a). By contrast, PLDζ2-GFP puncta barely overlapped with those of 2xmCherry-ATG8a (Fig. 3c). PLDζ2-GFP co-localized with VHP1-mCherry on large membrane structures (Fig. 3e), confirming that PLDζ2-GFP also localized to the tonoplast. Upon Wm treatment, PLDζ2-GFP localized to Wm-induced enlarged MVBs, where it formed ring-like structures, together with mRFP-ARA7 (Fig. 3j). These results consistently indicate that PLDζ2-GFP localizes not only to the tonoplast but also to ARA7-marked membrane compartments, including MVBs.

N-terminal partial proteins containing the PX-PH domains reproduced the subcellular localization patterns directed by PLDζ1 and PLDζ2

Next, we investigated protein regions that determine the subcellular localization patterns of PLDζ1 and PLDζ2. As the PX and PH domains interact with specific phospholipids and proteins on target membranes (Seet and Hong 2006; Lemmon 2007, 2008), we made constructs of N-terminal partial proteins, designated NPXPH1 and NPXPH2 (Supplementary Fig. S8), which consisted of the PX-PH domains and preceding N-terminal moieties, and expressed their fluorescence protein fusions using the *PLDζ1* and *PLDζ2* promoters, respectively. Transgenic plants harboring the transgenes *PLDζ1p-NPXPH1-mCitrine* and *PLDζ2p-NPXPH2-tdTomato* were established under the wild-type genetic background and then crossed with plants harboring *PLDζ1p-PLDζ1-mCherry* and *PLDζ2p-PLDζ2-GFP*, respectively. In mature lateral root cap cells, PLDζ1-mCherry and NPXPH1-mCitrine were strongly co-localized on punctate structures (Fig. 4a), and coincidence values between their signals were almost equal to the positive control values (Figs. 2p, 4c and Supplementary Fig. S6a, b). Similarly, PLDζ2-GFP and NPXPH2-tdTomato basically co-localized on the tonoplast and punctate structures (Fig. 4b), although the coincidence values for their punctate signals were slightly lower than values for the positive control (Figs. 3i, 4d and Supplementary Fig. S6c, d), possibly because their signal intensities were not strongly correlated in mature lateral root cap cells (Fig. 4b). These results strongly suggest that N-terminal regions containing the PX-PH domains are responsible for the subcellular localization patterns obtained under the direction of PLDζ1 and PLDζ2.

Inducibly overexpressed NPXPH1-mCitrine and NPXPH2-mCitrine localized first to punctate structures, and then partially or predominantly to the tonoplast

To comparatively investigate the protein regions responsible for subcellular localization, we expressed NPXPH1-mCitrine and NPXPH2-mCitrine using a common promoter. When the cauliflower mosaic virus 35S promoter was used for their expression, clear fluorescence signals for both fusion proteins were ubiquitous in root cap and root epidermal cells. However, their subcellular localization patterns

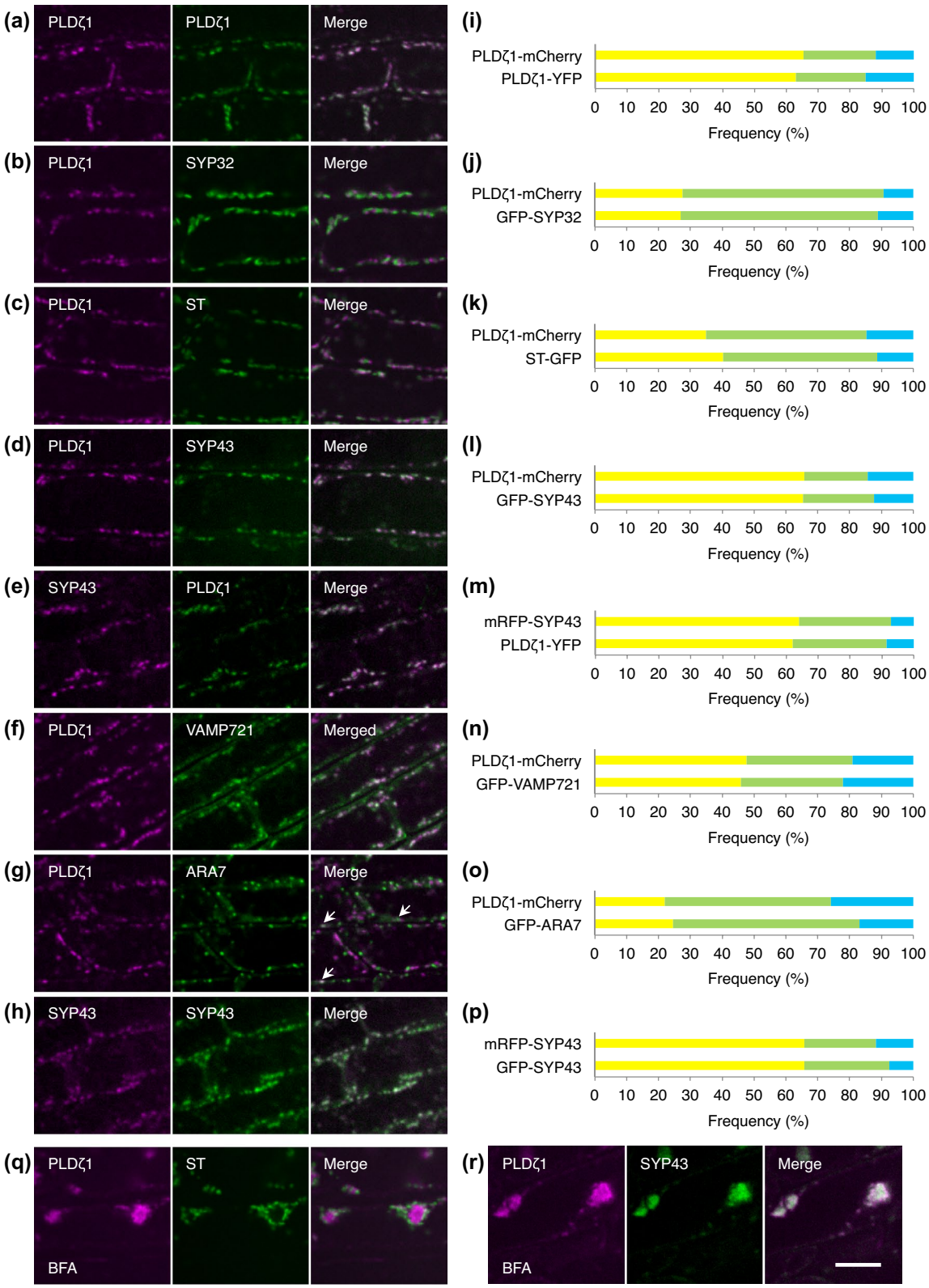
(a)
PLDζ1
PLDζ1
Merge
(b)
PLDζ1
SYP32
Merge
(c)
PLDζ1
ST
Merge
(d)
PLDζ1
SYP43
Merge
(e)
SYP43
PLDζ1
Merge
(f)
PLDζ1
VAMP721
Merged
(g)
PLDζ1
ARA7
Merge
(h)
SYP43
SYP43
Merge
(q)
PLDζ1
ST
Merge
BFA
(i)
PLDζ1-mCherry
PLDζ1-YFP
0 10 20 30 40 50 60 70 80 90 100
Frequency (%)
(j)
PLDζ1-mCherry
GFP-SYP32
0 10 20 30 40 50 60 70 80 90 100
Frequency (%)
(k)
PLDζ1-mCherry
ST-GFP
0 10 20 30 40 50 60 70 80 90 100
Frequency (%)
(l)
PLDζ1-mCherry
GFP-SYP43
0 10 20 30 40 50 60 70 80 90 100
Frequency (%)
(m)
mRFP-SYP43
PLDζ1-YFP
0 10 20 30 40 50 60 70 80 90 100
Frequency (%)
(n)
PLDζ1-mCherry
GFP-VAMP721
0 10 20 30 40 50 60 70 80 90 100
Frequency (%)
(o)
PLDζ1-mCherry
GFP-ARA7
0 10 20 30 40 50 60 70 80 90 100
Frequency (%)
(p)
mRFP-SYP43
GFP-SYP43
0 10 20 30 40 50 60 70 80 90 100
Frequency (%)
(r)
PLDζ1
SYP43
Merge
BFA

◂**Fig. 2** Subcellular localization analysis of PLDζ1-mCherry and PLDζ1-YFP in mature lateral root cap cells with membrane compartment markers. **a**–**h** Subcellular localization patterns of *PLDζ1* promoter-driven PLDζ1-mCherry and PLDζ1-YFP were compared with each other in mature lateral root cap cells (**a**). The pattern of PLDζ1-mCherry was compared with those of GFP-SYP32 (**b**), ST-mGFP (**c**), GFP-SYP43 (**d**), GFP-VAMP721 (**f**), and GFP-ARA7 (**g**). The pattern of PLDζ1-YFP was compared with that of mRFP-SYP43 (**e**). The patterns of co-expressed mRFP-SYP43 and GFP-SYP43 are shown in (**h**) as a positive control for co-localization. Images of mCherry or mRFP (magenta), GFP, mGFP, or YFP (green), and merged fluorescence signals are shown. Arrows in (**g**) indicate puncta to which both PLDζ1-mCherry and GFP-ARA7 co-localized. **i**–**p** The results of quantitative coincidence analysis of punctate structures containing different fluorescence signals are shown as in Fig. 1d. The quantified result of co-expressed mRFP-SYP43 and GFP-SYP43 is shown in (**p**) as a positive control for coincidence. The % values (mean ± SD, $n = 3$) of coincident puncta with the distance no more than 0.42 µm and results of statistical analysis are shown in Supplemental Fig. S6a, b. **q**, **r** The subcellular localization pattern of PLDζ1-mCherry driven by the *PLDζ1* promoter was compared with those of ST-mGFP (**b**) and GFP-SYP43 (**c**) in mature lateral root cap cells treated with 50 µM BFA for 20 min. Images of mCherry (magenta), GFP or mGFP (green), and merged fluorescence signals are shown. Bar = 10 µm

differed from those obtained under the original promoters, with partial and predominant localization to the tonoplast observed for NPXPH1-mCitrine and NPXPH2-mCitrine, respectively (Fig. 5a).

Next, we expressed the fusion proteins under the control of an estradiol-inducible system (Zuo et al. 2000), which allowed the timing and level of protein expression to be controlled. Fluorescence signals of both fusion proteins and their transcripts were detectable at 2 h after induction, and their total signal intensity and transcript levels increased over time (Fig. 5b, c, d). NPXPH1-mCitrine exhibited the same subcellular localization pattern as observed under the *PLDζ1* promoter from 2 to 4 h after induction (Fig. 5b). However, after 6 h, fluorescence signals were also detected on the tonoplast, and the pattern became aligned with that under the 35S promoter at 12 to 24 h after induction (Fig. 5a, b). NPXPH2-mCitrine was primarily localized to punctate structures at 2 h after induction, and increased in its signal intensity on the tonoplast over time (Fig. 5c), exhibiting almost the same localization pattern as under the *PLDζ2* promoter from 4 to 6 h after induction and a tonoplast-predominant pattern very similar to that observed with the 35S promoter at 12 to 24 h after induction (Fig. 5a, c). The punctate structures to which NPXPH2-mCitrine localized in the early period after induction were the same as those observed with own promoter-driven PLDζ2-GFP, which were marked with mRFP-ARA7 (Supplementary Figs. S6g, h, S9b, h). These results indicate that newly synthesized NPXPH2-mCitrine localized primarily to ARA7-marked compartments first, and that both NPXPH1-mCitrine and NPXPH2-mCitrine tended to accumulate on the tonoplast when overexpressed.

The N-terminal moiety of PLDζ2 drove NPXPH2-type tonoplast-predominant localization

To further characterize the protein regions required for subcellular localization, we created a series of mCitrine fusion constructs of chimeric and truncated N-terminal regions (Fig. 6a), and co-expressed them with NPXPH1-mCherry (Fig. 6b–i) or NPXPH2-mCherry (Fig. 6j–q), using the 35S promoter. All of the constructed fusion proteins exhibited one of two localization patterns, NPXPH1-type localization to punctate structures and the tonoplast or NPXPH2-type localization predominantly to the tonoplast. Chimeric proteins containing the PLDζ1 N-terminal moiety, NPX1/PH2-mCitrine and N1/PXPH2-mCitrine, exhibited almost identical localization to NPXPH1-mCherry (Fig. 6c, d, k, l). Reciprocally, those containing the PLDζ2 N-terminal moiety, NPX2/PH1-mCitrine and N2/PXPH1-mCitrine, exhibited almost identical localization to NPXPH2-mCherry pattern (Fig. 6f, g, n, o). These findings indicate that the selection of either the NPXPH1- or NPXPH2-type subcellular localization patterns depends not on the PX-PH domains but on the N-terminal moieties. However, both truncated proteins lacking the N-terminal moieties, PXPH1-mCitrine and PXPH2-mCitrine, exhibited the NPXPH1-type localization pattern (Fig. 6h, i, p, q). Together, these results indicate that the N-terminal moiety of PLDζ2 is required for the NPXPH2-type tonoplast-predominant localization, whereas either of the PX-PH domains alone can direct NPXPH1-type localization to punctate structures and the tonoplast when they are overexpressed. Truncated constructs without PH domains, NPX1-mCitrine and NPX2-mCitrin, expressed by the 35S promoter didn't exhibit any membrane localization patterns (Supplementary Fig. S10), suggesting that PH domains are indispensable for membrane localization of PLDζ1 and PLDζ2.

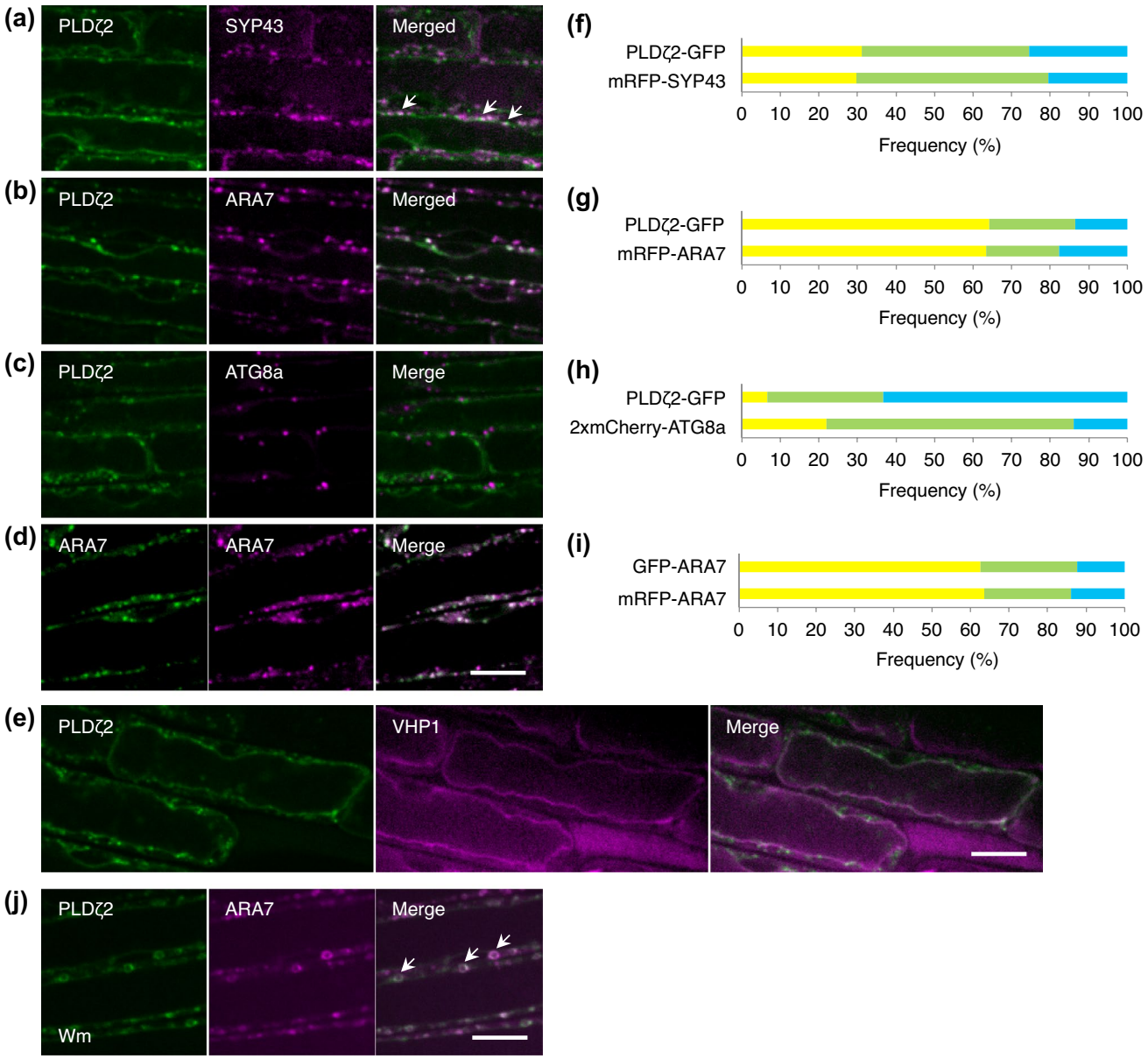

Fig. 3 Subcellular localization analysis of PLDζ2-GFP in mature lateral root cap cells with membrane compartment markers. **a**–**e** The subcellular localization pattern of PLDζ2-GFP driven by the *PLDζ2* promoter was compared with those of mRFP-SYP43 (**a**), mRFP-ARA7 (**b**), 2xmCherry-ATG8a (**c**), and VHP1-mCherry (**e**) in mature lateral root cap cells. The patterns of co-expressed GFP-ARA7 and mRFP-ARA7 are shown as a positive control for co-localization (**d**). Images of GFP (green), mRFP or mCherry (magenta), and merged fluorescence signals are shown. Arrows in (**a**) indicate puncta to which both PLDζ2-GFP and mRFP-SYP43 co-localized. **f**–**i** The results of quantitative coincidence analysis of punctate structures containing different fluorescence signals are shown as in Fig. 1d. The % values (mean ± SD, $n = 3$) of coincident puncta with the distance no more than 0.42 µm and results of statistical analysis are shown in Supplemental Fig. S6c and d. **j** The subcellular localization pattern of PLDζ2-GFP driven by the *PLDζ2* promoter was compared with that of mRFP-ARA7 in mature lateral root cap cells treated with 30 µM Wm for 1 h. Images of GFP (green), mRFP (magenta), and merged fluorescence signals are shown. Arrows indicate ring-like structures containing both mRFP and GFP fluorescence signals. Bar = 10 µm

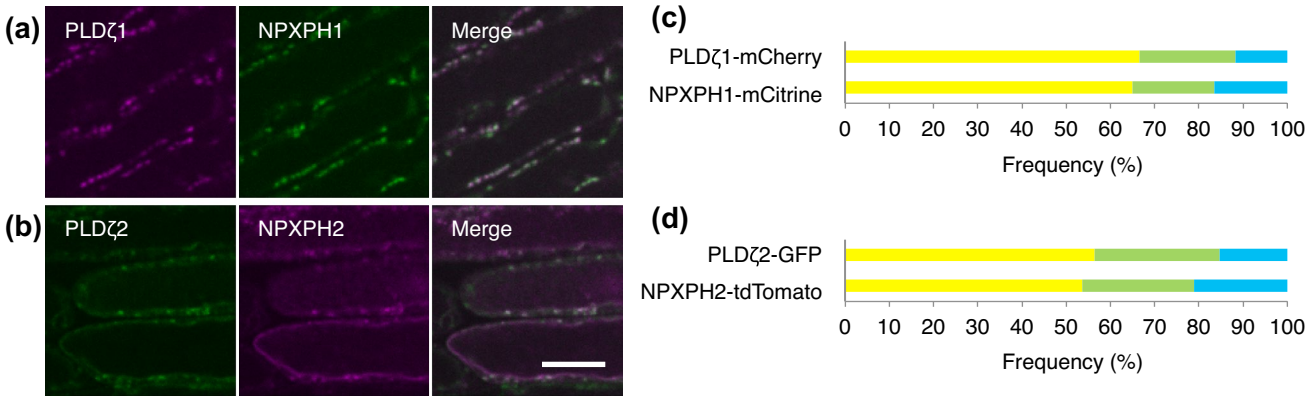

Fig. 4 Comparative analysis of subcellular localization between PLDζ1-mCherry and NPXPH1-mCitrine, and between PLDζ1-GFP and NPXPH2-tdTomato. **a**, **b** Subcellular localization patterns were compared between *PLDζ1* promoter-driven PLDζ1-mCherry and NPXPH1-mCitrine (**a**) and between *PLDζ2* promoter-driven PLDζ2-GFP and NPXPH2-tdTomato (**b**) in mature lateral root cap cells. Images of mCherry or tdTomato (magenta), mCitrine or GFP (green), and merged fluorescence signals are shown. **c**, **d** The results of quantitative coincidence analysis of punctate structures containing different fluorescence signals are shown as in Fig. 1d. The % values (mean ± SD, $n = 3$) of coincident puncta with the distance no more than 0.42 µm and results of statistical analysis are shown in Supplemental Fig. S6a–d. Bar = 10 µm

Discussion

We analyzed the subcellular localization of PLDζ1 and PLDζ2, and demonstrated that they localize to the TGN and to membrane compartments including a portion of the TGN, MVBs, and the tonoplast, respectively. For comparative analysis of their localization patterns, we observed mature lateral root cap cells, where both of their fluorescence protein fusions were expressed under their own promoters. We illustrated a model of subcellular localization for PLDζ1 and PLDζ2 (Fig. 7), in which PLDζ1 is localized throughout the TGN, whereas PLDζ2 is localized to compartments along the membrane trafficking pathway from the TGN to the tonoplast via MVBs in a pattern that partially overlaps with PLDζ1. In addition to recognizable membrane compartments, dispersed fluorescence signals from these fusion proteins were also detected in the cytoplasmic space, suggesting that PLDζ1 and PLDζ2 are diffusely present in the cytosol or on unrecognizably small vesicles.

Mammal PX-PH-PLDs, PLD1 and PLD2, localize to a wide variety of compartments including the plasma membrane, cytoplasmic organelles, and the nucleus (McDermott et al. 2020). On the other hand, PLDζ1 and PLDζ2 were found to localize to relatively specific compartments. Other plant PLDs, C2-PLDs, also show specific localization patterns in *Arabidopsis*, localizing to the cytoplasmic space in association with microtubules and clathrin-coated vesicles for PLDα1 (Novák et al. 2018), and to the plasma membrane for PLDγ1 (Schlöffel et al. 2020), PLDδ (Pinosa et al. 2013; Zhang et al. 2017, 2018; Xing et al. 2019), and PLDε (Hong et al. 2009). Plant PLDs may have specialized their subcellular localization patterns during evolutionary differentiation into the PX-PH- and C2-PLD types. However, because our analyses were performed using only roots grown under normal conditions, and because detectable levels for fluorescence signals were limited due to autofluorescence from plant compounds, it is possible that PLDζ1 and PLDζ2 may localize to compartments other than the ones observed in this study.

PLDζ1-mCherry and PLDζ1-YFP co-localized with GFP-SYP43 and mRFP-SYP43, respectively, while PLDζ2-GFP co-localized with mRFP-ARA7 on punctate structures. GFP-SYP43 and mRFP-ARA7 have been reported to partially overlap on punctate structures (Ito et al. 2016), and thus the partial overlap of PLDζ1-mCherry and PLDζ2-GFP is reasonable. However, coincidence values of punctate signals were relatively low between PLDζ1-mCherry and GFP-ARA7 (Fig. 2o and Supplementary Fig. S6a) and between PLDζ2-GFP and mRFP-SYP43 (Fig. 3e and Supplementary Fig. S6c) compared with between PLDζ1-mCherry and PLDζ2-GFP (Fig. 1d and Supplementary Fig. S6a, c), whereas partial co-localization was evidently observed between PLDζ1-mCherry and GFP-ARA7 (Fig. 2g) and between PLDζ2-GFP and mRFP-SYP43 (Fig. 3a). The loci where PLDζ1 and PLDζ2 overlap may differ slightly from the loci of SYP43 and ARA7.

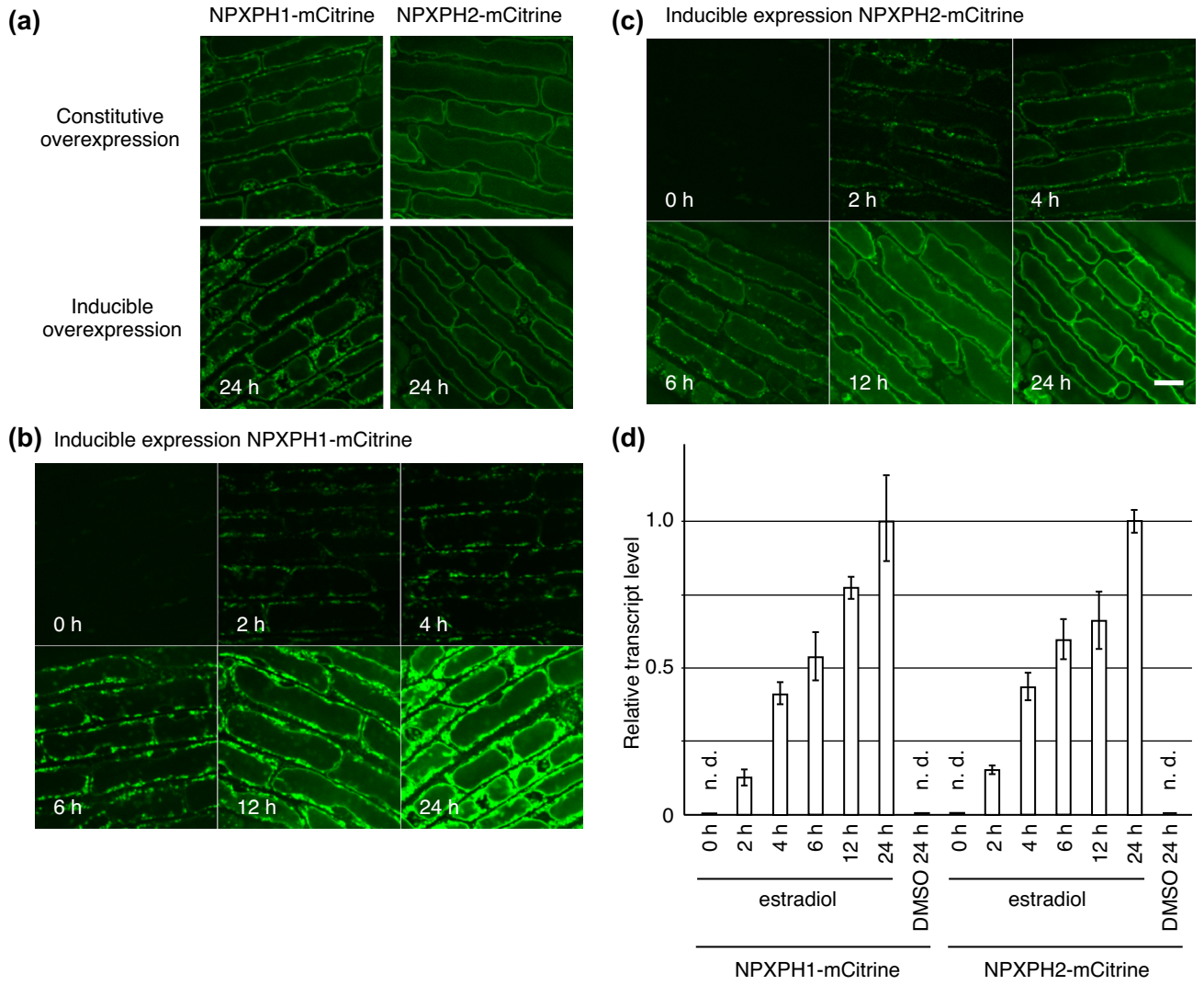

Fig. 5 Subcellular localization analysis of NPXPH1-mCitrine and NPXPH2-mCitrine using non-endogenous expression systems. **a** Subcellular localization patterns of NPXPH1-mCitrine and NPXPH2-mCitrine constitutively overexpressed by the cauliflower mosaic virus 35S promoter in mature lateral root cap cells are shown. For comparison with inducibly overexpressed NPXPH1-mCitrine and NPXPH2-mCitrine, the mages of 24-h induction shown in (**b**) and (**c**) are presented with lowered brightness. **b**, **c** Subcellular localization patterns of NPXPH1-mCitrine (**b**) and NPXPH2-mCitrine (**c**) expressed by an estradiol-inducible promoter were observed in mature lateral root cap cells. Images of fluorescence signals at 0, 2, 4, 6, 12, and 24 h after induction are shown. **d** Transcript levels of the NPXPH1-mCitrine and NPXPH2-mCitrine transgenes were determined by real-time RT-PCR. Relative transcript levels (means ± SD; $n = 3$) at indicated time points after the estradiol induction are shown with the mean value of the 24-h induction set as 1 for each transgene. The transcript levels in non-induced seedlings (DMSO 24 h) are shown as negative controls. n.d. indicates that relevant transcripts were not detected. Bars = 10 µm

The TGN, which also serves as an early endosome in plants, plays a pivotal role in sorting newly synthesized and endocytosed cargo and directing it to appropriate target compartments such as the plasma membrane and vacuoles (Uemura 2016; Reynolds et al. 2018; Rosquete et al. 2018). MVBs, which are also called as pre-vacuolar compartments or late endosomes, mediate membrane traffic from the TGN to vacuoles in their conventional function, and to autophagosomes and exosomes in recently revealed functions (Cui et al. 2016; Hansen and Nielsen 2018; Pečenková et al. 2018; Hu et al. 2020). Considering these functions, PA produced by PLDζ1 and PLDζ2 may be involved in membrane traffic via the TGN and via MVBs to the tonoplast, respectively. In particular, endocytic recycling and vacuolar degradation of plasma membrane proteins are crucial components of the mechanisms through which plant cells sense and respond to environmental stimuli. In accordance with

this concept, the involvement of PLDζ1 in endocytic recycling of the auxin efflux transporter PIN2 during root tropic responses has been reported (Korver et al. 2019).

PLDζ1-YFP has been reported to rescue the *pldζ1* phenotype of exaggerated root gravitropism (Korver et al. 2019). Meanwhile, PLDζ2-GFP rescued the *pldζ2* phenotype of retarded root gravitropism. These findings indicate that these fusion proteins retain the biological functions of their original proteins, at least in terms of root gravitropic responses, and suggest that their subcellular localization patterns are likely associated with these biological functions. Because lateral root cap cells serve as an auxin pathway for root gravitropism (Ottenschläger et al. 2003; Swarup et al. 2005), PLDζ1 and PLDζ2 in these cells may be involved in the root gravitropic responses either directly or indirectly through auxin flow. In addition to the presumed function of PLDζ1 in endocytic recycling of PIN2 (Korver et al. 2019), PLDζ2 may modulate the turnover of PIN2, which is transported through the TGN and MVBs for degradation in vacuoles (Kleine-Vehn et al. 2008; Spitzer et al. 2009). The result of our co-expression analysis with the programmed cell death marker gene *BFN1p-tdTomato* indicates that PLDζ2 is expressed near the distal end of lateral root cap cells, where the auxin flow that drives root gravitropism is redirected to root epidermal cells. Thus, PLDζ2 may be involved in auxin flow redirection via PIN2 turnover at the distal end of the lateral root cap. Previous studies have shown that promoters of the *PLDζ1* and *PLDζ2* genes are active in various cell types other than mature lateral root cap cells (Ohashi et al. 2003; Cruz-Ramírez et al. 2006; Li and Xue 2007; Taniguchi et al. 2010). In root tissues, while we observed basically the same localization pattern of own promoter-driven PLDζ1-YFP and PLDζ1-mCherry in various types of cells, including epidermal and cortex cells, own promoter-driven PLDζ2-GFP could be detected only in mature lateral root cap cells. PLDζ1 and PLDζ2 might be involved in root tissues-general and mature lateral root cap-specific cellular events, respectively.

We dissected the protein regions of PLDζ1 and PLDζ2 in terms of their subcellular localization, and found that N-terminal partial proteins containing the PX-PH domains reproduced the patterns of the full-length proteins when their own promoters were used. This result strongly suggests that the N-terminal regions containing PX-PH domains are the determinants of subcellular localization for PLDζ1 and PLDζ2. However, considering the dimerization ability of mammalian PLDs (Kam et al., 2002), the possibility can't be excluded that NPXPH1 and NPXPH2 localized dependently on heterodimerization with the endogenous PLDζ1 and PLDζ2, while it remains unknown whether the reported dimerization activity belongs to the PX-PH domain. T-DNA insertion mutants of the *PLDζ1* and *PLDζ2* genes might produce partial protein products that retain abilities for dimerization and subcellular localization. Inducibly expressed NPXPH2-YFP exhibited the same co-localization pattern with mRFP-ARA7 in root epidermal cells, where endogenous PLDζ2 are not expressed, as in mature lateral root cap cells (Supplementary Figs. S6g, h and S9b, h, e, k), indicating at least that the NPXPH2 localization is independent of endogenous PLDζ2.

The PX and PH domains of mammal PLDs PLD1 and PLD2 also play pivotal roles in their subcellular localization (McDermott et al. 2020). In addition to various protein targets, the PH domains of both PLD1 and PLD2 preferentially interact with phosphatidylinositol 4,5-bisphosphate (Hodgkin et al. 2000; Sciorra et al. 2002), whereas the PX domain of PLD1, but not that of PLD2, specifically interacts with phosphatidylinositol 3,4,5-trisphosphate (Stahelin et al. 2004; Lee et al. 2005). As for the PX-PH domains of PLDζ1 and PLDζ2, it is difficult to identify specific targets among the wide variety of molecules that may interact with the PX and PH domains (Seet and Hong 2006; Lemmon 2007, 2008). Notably, the N-terminal moiety of PLDζ2 exhibited a dominant function in tonoplast-predominant localization. While we can't find any functional motifs in its short amino-acid sequence, it may modulate interactions between the PX-PH domains and regulatory molecules for subcellular localization. Experimental evidence is needed to identify the target molecules of the PX-PH domains that drive subcellular localization.

When the 35S promoter was used as a common promoter for comparative analysis, fluorescence protein fusions of NPXPH1 and NPXPH2 localized partially and predominantly to the tonoplast, respectively. The tonoplast-predominant pattern of NPXPH2 closely aligns with the reported distribution of PLDζ2 and its N-terminal partial protein under the 35S promoter (Yamaryo et al. 2008). The tonoplast-predominant localization pattern might reflect localizations of endogenous PLDζ1 and PLDζ2 under stressed conditions that greatly enhance their expression levels, such as phosphate starvation. Because the tonoplast-predominant localization was accompanied by overexpression in inducible expression analysis, these proteins are likely to accumulate on the tonoplast when overexpressed. Intriguingly, NPXPH2-mCitrine localized mainly to ARA7-marked compartments shortly after induction. Further comparative dissection analysis revealed that the N-terminal moiety of PLDζ2 is required for tonoplast-predominant accumulation. Based on these results, we hypothesize that newly synthesized PLDζ2 is recruited to membrane compartments including part of the TGN and MVBs, and then transferred to the tonoplast depending on the N-terminal moiety (Fig. 7).

The subcellular localization patterns of PLDζ1 and PLDζ2 revealed in this study suggest that they play partially overlapping but nonetheless distinctive roles in post-Golgi

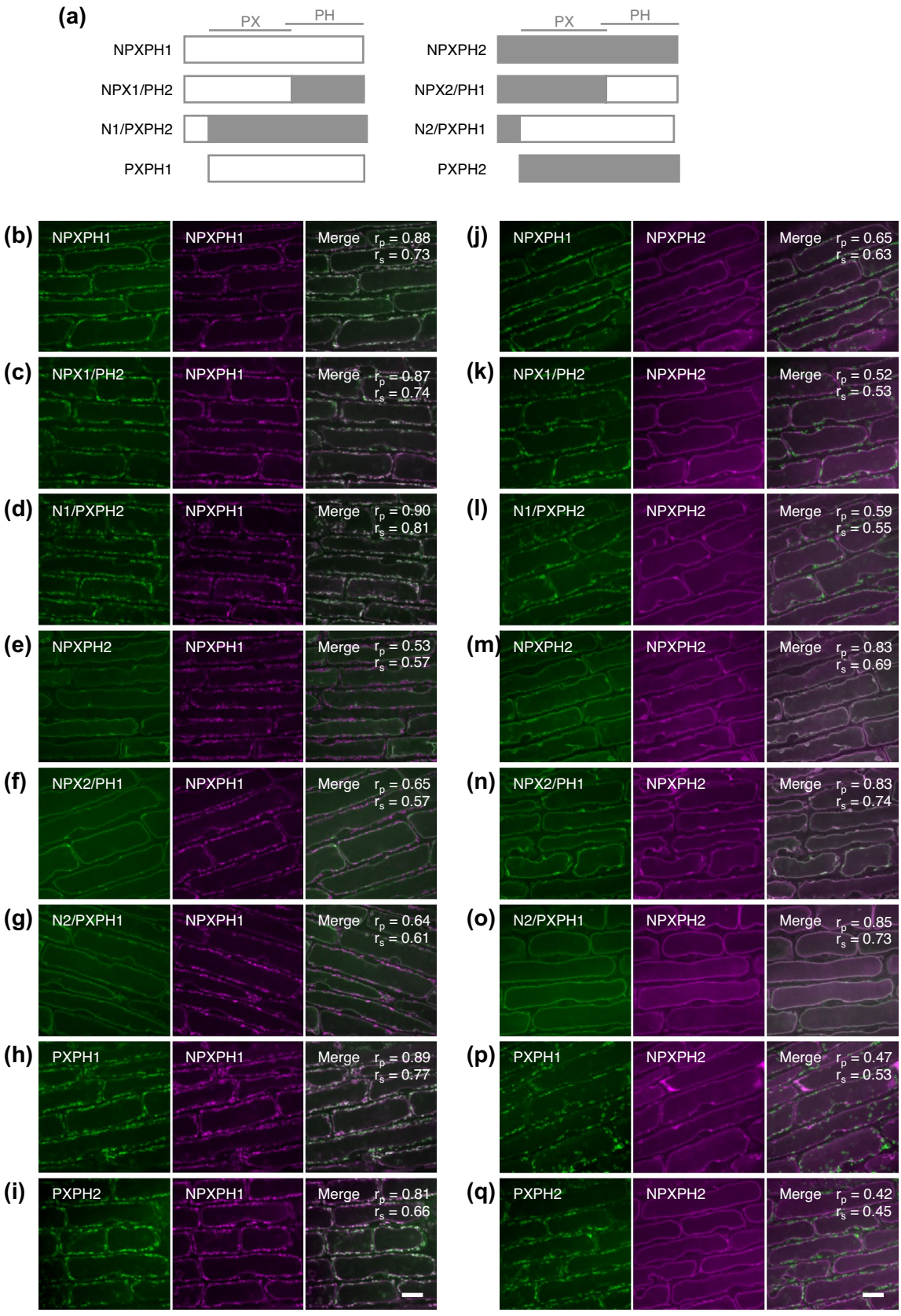
(a)
PX
PH
NPXPH1
NPX1/PH2
N1/PXPH2
PXPH1
NPXPH2
NPX2/PH1
N2/PXPH1
PXPH2
(b) NPXPH1 NPXPH1 Merge r_p = 0.88 r_s = 0.73
(c) NPX1/PH2 NPXPH1 Merge r_p = 0.87 r_s = 0.74
(d) N1/PXPH2 NPXPH1 Merge r_p = 0.90 r_s = 0.81
(e) NPXPH2 NPXPH1 Merge r_p = 0.53 r_s = 0.57
(f) NPX2/PH1 NPXPH1 Merge r_p = 0.65 r_s = 0.57
(g) N2/PXPH1 NPXPH1 Merge r_p = 0.64 r_s = 0.61
(h) PXPH1 NPXPH1 Merge r_p = 0.89 r_s = 0.77
(i) PXPH2 NPXPH1 Merge r_p = 0.81 r_s = 0.66
(j) NPXPH1 NPXPH2 Merge r_p = 0.65 r_s = 0.63
(k) NPX1/PH2 NPXPH2 Merge r_p = 0.52 r_s = 0.53
(l) N1/PXPH2 NPXPH2 Merge r_p = 0.59 r_s = 0.55
(m) NPXPH2 NPXPH2 Merge r_p = 0.83 r_s = 0.69
(n) NPX2/PH1 NPXPH2 Merge r_p = 0.83 r_s = 0.74
(o) N2/PXPH1 NPXPH2 Merge r_p = 0.85 r_s = 0.73
(p) PXPH1 NPXPH2 Merge r_p = 0.47 r_s = 0.53
(q) PXPH2 NPXPH2 Merge r_p = 0.42 r_s = 0.45

◂**Fig. 6** Comparative dissection analysis of functional protein regions of NPXPH1 and NPXPH2 for subcellular localization. **a** Chimeric protein constructs between NPXPH1 and NPXPH2, and truncated protein constructs are schematically illustrated. Open and filled boxes indicate protein regions originating from PLDζ1 and PLDζ2, respectively. Upper lines indicate regions corresponding to the PX and PH domains. **b**–**q** mCitrine-fused protein constructs shown in (**a**) were co-expressed with NPXPH1-mCherry (**b**–**i**) or NPXPH2-mCherry (**j**–**q**) by the 35S promoter, and observed in mature lateral root cap cells. Images of mCitrine (green), mCherry (magenta), and merged fluorescence signals are shown. Values of the linear Pearson correlation coefficient (r_p) and the non-linear Spearman's rank (r_s) between pairs of fluorescence images are presented in merged images. Bars = 10 µm

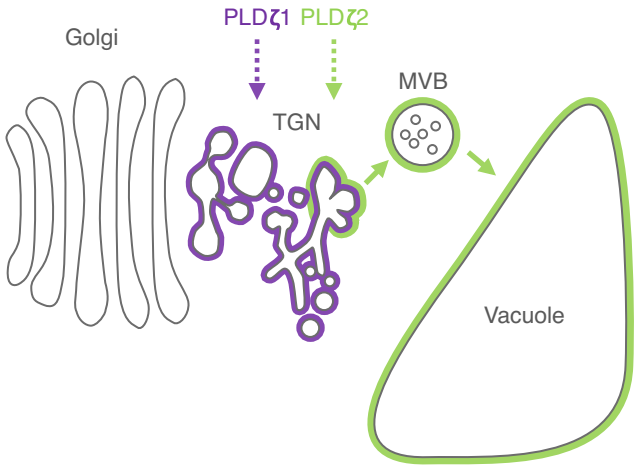

Fig. 7 Model for subcellular localizations of PLDζ1 and PLDζ2. Hypothesized subcellular localization patterns of PLDζ1 and PLDζ2 are schematically illustrated. Membrane compartments containing PLDζ1 and PLDζ2 are outlined in magenta and green, respectively. Dashed arrows indicate recruitment of newly synthesized PLDζ1 and PLDζ2 to membrane compartments. Solid arrows indicate transfer of PLDζ2 between membrane compartments. PLDζ1 and PLDζ2 mainly localize to the TGN and compartments including part of the TGN, MVBs, and the tonoplast, respectively, in a partially overlapping manner. They may also localize to unrecognizable compartments in the cytoplasmic space. Newly synthesized PLDζ2 is recruited to membrane compartments including part of TGN and MVBs, and transferred to the tonoplast

compartments along the membrane trafficking pathway from the TGN to the tonoplast rather than in signal transduction on the plasma membrane. To verify this hypothesis, spatiotemporal analyses of PLDζ1 and PLDζ2 functioning in membrane trafficking are needed. In future studies, it will be essential to identify the target molecules of PLDζ1 and PLDζ2 that determine their subcellular localization and to analyze their dynamic interactions with these molecules.

Supplementary Information The online version contains supplementary material available at https://doi.org/10.1007/s11103-021-01205-0.

Acknowledgements We are grateful to Ms. Keiko Yasuda (Kyoto University) for technical assistance, Dr. Christa Testerink for providing transgenic seeds of the *pPLDζ1::PLDζ1-YFP* line, Dr. Yasuo Niwa for the GFP-coding fragment, Dr. Takashi Ueda for seeds of the marker lines of GFP-SYP32, GFP-SYP43, GFP-VAMP721, GFP-ARA7, and mRFP-ARA7, Dr. Tomohiro Uemura for seeds of the marker line of mRFP-SYP43, and Dr. Masayoshi Maeshima for the plasmid vector pENTR-VHP1-mGFP.

Author Contributions RS conceived the study, designed the experiments, performed the research, analyzed the data, and prepared the manuscript. YO, YYT, MK, and TT contributed to experimental design and analyzed the data. TA contributed to experimental design, data analysis and manuscript preparation, and submitted the manuscript.

Funding This work was supported by Grants-in-Aid for Scientific Research (KAKENHI) from the Japanese Society for the Promotion of Science (JSPS); 16H04804 to T.A, the International Collaborative Research Program of the Institute for Chemical Research, Kyoto University; #202064 to Y.O., and Kyoto University Education and Research Foundation and ISHIZUE 2020 of Kyoto University Research Development Program to M.K.

Data availability All data generated and analyzed during this study are included in the article and its supplementary information files. Plasmids, mutants, and transgenic lines are available upon request.

Code availability No applicable.

Declarations

Conflict of interest The authors declare no conflict of interest/competing interests.

Ethical approval No applicable.

Consent to participate No applicable.

Consent for publication No applicable.

References

Alonso JM, Stepanova AN, Leisse TJ et al (2003) Genome-wide insertional mutagenesis of *Arabidopsis thaliana*. Science 301:653–657. https://doi.org/10.1126/science.1086391

Athenstaedt K, Daum G (1999) Phosphatidic acid, a key intermediate in lipid metabolism. Eur J Biochem 266:1–16. https://doi.org/10.1046/j.1432-1327.1999.00822.x

Bankaitis VA, Garcia-Mata R, Mousley CJ (2012) Golgi membrane dynamics and lipid metabolism. Curr Biol 22:R414–R424. https://doi.org/10.1016/j.cub.2012.03.004

Bargmann BOR, Laxalt AM, ter Riet B, van Schooten B, Merquiol E, Testerink C, Haring MA, Bartels D, Munnik T (2009) Multiple PLDs required for high salinity and water deficit tolerance in plants. Plant Cell Physiol 50:78–89. https://doi.org/10.1093/pcp/pcn173

Boevink P, Oparka K, Cruz SS, Martin B, Betteridge A, Hawes C (1998) Stacks on tracks: the plant Golgi apparatus traffics on an actin/ER network. Plant J 15:441–447. https://doi.org/10.1046/j.1365-313x.1998.00208.x

Camehl I, Drzewiecki C, Vadassery J, Shahollari B, Sherameti I, Forzani C, Munnik T, Hirt H, Oelmüller R (2011) The OXI1 kinase pathway mediates *Piriformospora indica*-induced growth promotion in *Arabidopsis*. PLoS Pathog 7:e1002051. https://doi.org/10.1371/journal.ppat.1002051

Chen G, Greer MS, Weselake RJ (2013) Plant phospholipase A: advances in molecular biology, biochemistry, and cellular function. Biomol Concepts 4:527–532. https://doi.org/10.1515/bmc-201300011

Chiu W, Niwa Y, Zeng W, Hirano T, Kobayashi H, Sheen J (1996) Engineered GFP as a vital reporter in plants. Curr Biol 6:325–330. https://doi.org/10.1016/s0960-9822(02)00483-9

Clough SJ, Bent AF (1998) Floral dip: a simplified method for *Agrobacterium*-mediated transformation of *Arabidopsis thaliana*. Plant J 16:735–743. https://doi.org/10.1046/j.1365-313x.1998.00343.x

Cruz-Ramirez A, Oropeza-Aburto A, Razo-Hernandez F, Ramirez-Chavez E, Herrera-Estrella L (2006) Phospholipase DZ2 plays an important role in extraplastidic galactolipid biosynthesis and phosphate recycling in *Arabidopsis* roots. Proc Natl Acad Sci USA 103:6765–6770. https://doi.org/10.1073/pnas.0600863103

Cui Y, Shen J, Gao C, Zhuang X, Wang J, Jiang L (2016) Biogenesis of plant prevacuolar multivesicular bodies. Mol Plant 9:774–786. https://doi.org/10.1016/j.molp.2016.01.011

Distéfano AM, Valiñas MA, Scuffi D, Lamattina L, ten Have A, García-Mata C, Laxalt AM (2015) Phospholipase D δ knock-out mutants are tolerant to severe drought stress. Plant Signal Behav 10:e1089371. https://doi.org/10.1080/15592324.2015.1089371

Donaldson JG (2009) Phospholipase D in endocytosis and endosomal recycling pathways. Biochim Biophys Acta 1791:845–849. https://doi.org/10.1016/j.bbalip.2009.05.011

Eliáš M, Potocký M, Cvrčková F, Žárský V (2002) Molecular diversity of phospholipase D in angiosperms. BMC Genom 3:2. https://doi.org/10.1186/1471-2164-3-2

Fendrych M, Van Hautegem T, Van Durme M, Olvera-Carrillo Y, Huysmans M, Karimi M, Lippens S, Guérin CJ, Krebs M, Schumacher K, Nowack MK (2014) Programmed cell death controlled by ANAC033/SOMBRERO determines root cap organ size in *Arabidopsis*. Curr Biol 24:931–940. https://doi.org/10.1016/j.cub.2014.03.025

Filkin SY, Lipkin AV, Fedorov AN (2020) Phospholipase super family: structure, functions, and biotechnological applications. Biochemistry (Mosc) 85(Suppl 1):S177–S195. https://doi.org/10.1134/S0006297920140096

Frohman MA, Morris AJ (1999) Phospholipase D structure and regulation. Chem Phys Lipids 98:127–140. https://doi.org/10.1016/s0009-3084(99)00025-0

Galvan-Ampudia CS, Julkowska MM, Darwish E, Gandullo J, Korver RA, Brunoud G, Haring MA, Munnik T, Vernoux T, Testerink C (2013) Halotropism is a response of plant roots to avoid a saline environment. Curr Biol 23:2044–2050. https://doi.org/10.1016/j.cub.2013.08.042

Gao HB, Chu YJ, Xue HW (2013) Phosphatidic acid (PA) binds PP2AA1 to regulate PP2A activity and PIN1 polar localization. Mol Plant 6:1692–1702. https://doi.org/10.1093/mp/sst076

Geldner N, Dénervaud-Tendon V, Hyman DL, Mayer U, Stierhof YD, Chory J (2009) Rapid, combinatorial analysis of membrane compartments in intact plants with a multicolor marker set. Plant J 59:169–178. https://doi.org/10.1111/j.1365-313X.2009.03851.x

Griesbeck O, Baird GS, Campbell RE, Zacharias DA, Tsien RY (2001) Reducing the environmental sensitivity of yellow fluorescent protein. J Biol Chem 276:29188–29194. https://doi.org/10.1074/jbc.M102815200

Guo L, Devaiah SP, Narasimhan R, Pan X, Zhang Y, Zhang W, Wang X (2012) Cytosolic glyceraldehyde-3-phosphate dehydrogenases interact with phospholipase Dδ to transduce hydrogen peroxide signals in the *Arabidopsis* response to stress. Plant Cell 24:2200–2212. https://doi.org/10.1105/tpc.111.094946

Hansen LL, Nielsen ME (2018) Plant exosomes: using an unconventional exit to prevent pathogen entry? J Exp Bot 69:59–68. https://doi.org/10.1093/jxb/erx319

Hodgkin MN, Masson MR, Powner D, Saqib KM, Ponting CP, Wakelam MJO (2000) Phospholipase D regulation and localisation is dependent upon a phosphatidylinositol 4,5-bisphosphate-specific PH domain. Curr Biol 10:43–46. https://doi.org/10.1016/s0960-9822(99)00264-x

Hong Y, Pan X, Welti R, Wang X (2008) Phospholipase Dα3 Is involved in the hyperosmotic response in *Arabidopsis*. Plant Cell 20:803–816. https://doi.org/10.1105/tpc.107.056390

Hong Y, Devaiah SP, Bahn SC, Thamasandra BN, Li M, Welti R, Wang X (2009) Phospholipase Dε and phosphatidic acid enhance *Arabidopsis* nitrogen signaling and growth. Plant J 58:376–387. https://doi.org/10.1111/j.1365-313X.2009.03788.x

Hong Y, Zhao J, Guo L, Kim SC, Deng X, Wang G, Zhang G, Li M, Wang X (2016) Plant phospholipases D and C and their diverse functions in stress responses. Prog Lipid Res 62:55–74. https://doi.org/10.1016/j.plipres.2016.01.002

Hu S, Li Y, Shen J (2020) A diverse membrane interaction network for plant multivesicular bodies: roles in proteins vacuolar delivery and unconventional secretion. Front Plant Sci 11:425. https://doi.org/10.3389/fpls.2020.00425

Ito E, Uemura T, Ueda T, Nakano A (2016) Distribution of RAB5-positive multivesicular endosomes and the *trans*-Golgi network in root meristematic cells of *Arabidopsis thaliana*. Plant Biotechnol (Tokyo) 33:281–286. https://doi.org/10.5511/plantbiotechnology.16.0218a

Jenkins GM, Frohman MA (2005) Phospholipase D: a lipid centric review. Cell Mol Life Sci 62:2305–2316. https://doi.org/10.1007/s00018-005-5195-z

Johansson ON, Fahlberg P, Karimi E, Nilsson AK, Ellerström M, Andersson MX (2014) Redundancy among phospholipase D isoforms in resistance triggered by recognition of the *Pseudomonas syringae* effector AvrRpm1 in *Arabidopsis thaliana*. Front Plant Sci 5:639. https://doi.org/10.3389/fpls.2014.00639

Kam Y, Exton J (2002) Dimerization of phospholippase D isozymes. Biochem Biophys Res Comm 290:375–380. https://doi.org/10.1006/bbrc.2001.6146

Kleine-Vehn J, Leitner J, Zwiewka M, Sauer M, Abas L, Friml LC, J, (2008) Differential degradation of PIN2 auxin efflux carrier by retromer-dependent vacuolar targeting. Proc Natl Acad Sci USA 105:17812–17817. https://doi.org/10.1073/pnas.0808073105

Kolesnikov YS, Nokhrina KP, Kretynin SV, Volotovski ID, Martinec J, Romanov GA, Kravets VS (2012) Molecular structure of phospholipase D and regulatory mechanisms of its activity in plant and animal cells. Biochemistry 77:1–14. https://doi.org/10.1134/S0006297912010014

Kooijman EE, Chupin V, de Kruijff B, Burger KNJ (2003) Modulation of membrane curvature by phosphatidic acid and lysophosphatidic acid. Traffic 4:162–174. https://doi.org/10.1034/j.1600-0854.2003.00086.x

Korver RA, Berg T, Meyer AJ, Galvan-Ampudia CS, Tusscher KHWJ, Testerink C (2019) Halotropism requires phospholipase Dζ1-mediated modulation of cellular polarity of auxin transport carriers. Plant Cell Environ 43:143–158. https://doi.org/10.1111/pce.13646

Kotzer AM, Brandizzi F, Neumann U, Paris N, Moore I, Hawes C (2004) *At*RabF2b (Ara7) acts on the vacuolar trafficking pathway in tobacco leaf epidermal cells. J Cell Sci 117:6377. https://doi.org/10.1242/jcs.01564

Kusano H, Testerink C, Vermeer JEM, Tsuge T, Shimada H, Oka A, Munnik T, Aoyama T (2008) The *Arabidopsis*

phosphatidylinositol phosphate 5-kinase PIP5K3 is a key regulator of root hair tip growth. Plant Cell 20:367–380. https://doi.org/10.1105/tpc.107.056119

Lee GJ, Sohn EJ, Lee MH, Hwang I (2004) The *Arabidopsis* Rab5 homologs Rha1 and Ara7 localize to the prevacuolar compartment. Plant Cell Physiol 45:1211–1220. https://doi.org/10.1093/pcp/pch142

Lee JS, Kim JH, Jang IH, Kim HS, Han JM, Kazlauskas A, Hitoshi Y, Suh PG, Ryu SH (2005) Phosphatidylinositol (3,4,5)-trisphosphate specifically interacts with the phox homology domain of phospholipase D1 and stimulates its activity. J Cell Sci 118:4405–4413. https://doi.org/10.1242/jcs.02564

Lemmon MA (2007) Pleckstrin homology (PH) domains and phosphoinositides. Biochem Soc Symp 74:81–93. https://doi.org/10.1042/BSS0740081

Lemmon MA (2008) Membrane recognition by phospholipid-binding domains. Nat Rev Mol Cell Biol 9:99–111. https://doi.org/10.1038/nrm2328

Li J, Wang X (2019) Phospholipase D and phosphatidic acid in plant immunity. Plant Sci 279:45–50. https://doi.org/10.1016/j.plantsci.2018.05.021

Li G, Xue HW (2007) *Arabidopsis PLDζ2* regulates vesicle trafficking and is required for auxin response. Plant Cell 19:281–295. https://doi.org/10.1105/tpc.106.041426

Li W, Li M, Zhang W, Welti R, Wang X (2004) The plasma membrane–bound phospholipase Dδ enhances freezing tolerance in *Arabidopsis thaliana*. Nat Biotechnol 22:427–433. https://doi.org/10.1038/nbt949

Li M, Qin C, Welti R, Wang X (2006) Double knockouts of phospholipases Dζ1 and Dζ2 in Arabidopsis affect root elongation during phosphate-limited growth but do not affect root hair patterning. Plant Physiol 140:761–770. https://doi.org/10.1104/pp.105.070995

Li M, Welti R, Wang X (2006) Quantitative profiling of Arabidopsis polar glycerolipids in response to phosphorus starvation. Roles of phospholipases Dζ1 and Dζ2 in phosphatidylcholine hydrolysis and digalactosyldiacylglycerol accumulation in phosphorus-starved plants. Plant Physiol 142:750–761. https://doi.org/10.1104/pp.106.085647

Li M, Hong Y, Wang X (2009) Phospholipase D- and phosphatidic acid-mediated signaling in plants. Biochim Biophys Acta 1791:927–935. https://doi.org/10.1016/j.bbalip.2009.02.017

Lin DL, Yao HY, Jia LH, Tan JF, Xu ZH, Zheng WM, Xue HW (2020) Phospholipase D-derived phosphatidic acid promotes root hair development under phosphorus deficiency by suppressing vacuolar degradation of PIN-FORMED2. New Phytol 226:142–155. https://doi.org/10.1111/nph.16330

Liscovitch M, Czarny M, Fiucci G, Tang X (2000) Phospholipase D: molecular and cell biology of a novel gene family. Biochem J 345:401–415. https://doi.org/10.1042/bj3450401

McDermott MI, Wang Y, Wakelam MJO, Bankaitis VA (2020) Mammalian phospholipase D: function, and therapeutics. Prog Lipid Res 78:101018. https://doi.org/10.1016/j.plipres.2019.101018

McLoughlin F, Testerink C (2013) Phosphatidic acid, a versatile water-stress signal in roots. Front Plant Sci 4:525. https://doi.org/10.3389/fpls.2013.00525

McMahon HT, Gallop JL (2005) Membrane curvature and mechanisms of dynamic cell membrane remodelling. Nature 438:590–596. https://doi.org/10.1038/nature04396

Michniewicz M, Zago MK, Abas L, Weijers D, Schweighofer A, Meskiene I, Heisler MG, Ohno C, Zhang J, Huang F, Schwab R, Weigel D, Meyerowitz EM, Luschnig C, Offringa R, Friml J (2007) Antagonistic regulation of PIN phosphorylation by PP2A and PINOID directs auxin flux. Cell 130:1044–1056. https://doi.org/10.1016/j.cell.2007.07.033

Mishra G, Zhang W, Deng F, Wang X (2006) A bifurcating pathway directs abscisic acid effects on stomatal closure and opening in *Arabidopsis*. Science 312:264–266. https://doi.org/10.1126/science.1123769

Munnik T (2001) Phosphatidic acid: an emerging plant lipid second messenger. Trends Plant Sci 6:227–233. https://doi.org/10.1016/s1360-1385(01)01918-5

Munnik T (2014) PI-PLC: phosphoinositide-phospholipase C in plant signaling. In: Wang S (ed) Phospholipase in plant signaling. Springer, Heidelberg, pp 27–54

Murashige T, Skoog F (1962) A revised medium for rapid growth and bio assays with tobacco tissue cultures. Physiol Plant 15:473–497. https://doi.org/10.1111/j.1399-3054.1962.tb08052.x

Nakamura Y (2014) NPC: Nonspecific phospholipase Cs in plant functions. In: Wang S (ed) Phospholipase in plant signaling. Springer, Heidelberg, pp 43–50

Novák D, Vadovič P, Ovečka M, Šamajová O, Komis G, Colcombet J, Šamaj J (2018) Gene expression pattern and protein localization of Arabidopsis phospholipase D alpha 1 revealed by advanced light-sheet and super-resolution microscopy. Front Plant Sci 9:371. https://doi.org/10.3389/fpls.2018.00371

Ohashi Y, Oka A, Rodrigues-Pousada R, Possenti M, Ruberti I, Morelli G, Aoyama T (2003) Modulation of phospholipid signaling by GLABRA2 in root-hair pattern formation. Science 300:1427–1430. https://doi.org/10.1126/science.1083695

Ottenschläger I, Wolff P, Wolverton C, Bhalerao RP, Sandberg G, Ishikawa H, Evans M, Palme K (2003) Gravity-regulated differential auxin transport from columella to lateral root cap cells. Proc Natl Acad Sci USA 100:2987–2991. https://doi.org/10.1073/pnas.0437936100

Pečenková T, Marković V, Sabol P, Kulich I, Žárský V (2018) Exocyst and autophagy-related membrane trafficking in plants. J Exp Bot 69:47–57. https://doi.org/10.1093/jxb/erx363

Pinosa F, Buhot N, Kwaaitaal M, Fahlberg P, Thordal-Christensen H, Ellerström M, Andersson MX (2013) *Arabidopsis* phospholipase D is involved in basal defense and nonhost resistance to powdery mildew fungi. Plant Physiol 163:896–906. https://doi.org/10.1104/pp.113.223503

Pleskot R, Li J, Žárský V, Potocký M, Staiger CJ (2013) Regulation of cytoskeletal dynamics by phospholipase D and phosphatidic acid. Trends Plant Sci 18:496–504. https://doi.org/10.1016/j.tplants.2013.04.005

Pokotylo I, Kravets V, Martinec J, Ruelland E (2018) The phosphatidic acid paradox: too many actions for one molecule class? Lessons from plants. Prog Lipid Res 71:43–53. https://doi.org/10.1016/j.plipres.2018.05.003

Qin C, Wang X (2002) The Arabidopsis phospholipase D family. Characterization of a calcium-independent and phosphatidylcholine-selective PLDζ1 with distinct regulatory domains. Plant Physiol 128:1057–1068. https://doi.org/10.1104/pp.010928

Raghu P, Manifava M, Coadwell J, Ktistakis NT (2009) Emerging findings from studies of phospholipase D in model organisms (and a short update on phosphatidic acid effectors). Biochim Biophys Acta 1791:889–897. https://doi.org/10.1016/j.bbalip.2009.03.013

Reynolds GD, Wang C, Pan J, Bednarek SY (2018) Inroads into internalization: five years of endocytic exploration. Plant Physiol 176:208–218. https://doi.org/10.1104/pp.17.01117

Rosquete MR, Davis DJ, Drakakaki G (2018) The plant trans-Golgi network: not just a matter of distinction. Plant Physiol 176:187–198. https://doi.org/10.1104/pp.17.01239

Roth MG (2008) Molecular mechanisms of PLD function in membrane traffic. Traffic 9:1233–1239. https://doi.org/10.1111/j.1600-0854.2008.00742.x

Schlöffel MA, Salzer A, Wan WL, van Wijk R, Del Corvo R, Šemanjski M, Symeonidi E, Slaby P, Kilian J, Maček B, Munnik T, Gust

AA (2020) The BIR2/BIR3-associated phospholipase Dγ1 negatively regulates plant immunity. Plant Physiol 183:371–384. https://doi.org/10.1104/pp.19.01292

Sciorra VA, Rudge SA, Wang J, McLaughlin S, Engebrecht J, Morris AJ (2002) Dual role for phosphoinositides in regulation of yeast and mammalian phospholipase D enzymes. J Cell Biol 159:1039–1049. https://doi.org/10.1083/jcb.200205056

Seet LF, Hong W (2006) The phox (PX) domain proteins and membrane traffic. Biochim Biophys Acta 1761:878–896. https://doi.org/10.1016/j.bbalip.2006.04.011

Segami S, Makino S, Miyake A, Asaoka M, Maeshima M (2014) Dynamics of vacuoles and H^+-pyrophosphatase visualized by monomeric green fluorescent protein in *Arabidopsis*. Plant Cell 26:3416–3434. https://doi.org/10.1105/tpc.114.127571

Spitzer C, Reyes FC, Buono R, Sliwinski MK, Haas TJ, Otegui MS (2009) The ESCRT-related CHMP1A and B Proteins mediate multivesicular body sorting of auxin carriers in *Arabidopsis* and are required for plant development. Plant Cell 21:749–766. https://doi.org/10.1105/tpc.108.064865

Stace CL, Ktistakis NT (2006) Phosphatidic acid- and phosphatidylserine-binding proteins. Biochim Biophys Acta 1761:913–926. https://doi.org/10.1016/j.bbalip.2006.03.006

Stahelin RV, Ananthanarayanan B, Blatner NR, Singh S, Bruzik KS, Murray D, Cho W (2004) Mechanism of membrane binding of the phospholipase D1 PX domain. J Biol Chem 279:54918–54926. https://doi.org/10.1074/jbc.M407798200

Su Y, Li M, Guo L, Wang X (2018) Different effects of phospholipase Dζ2 and non-specific phospholipase C4 on lipid remodeling and root hair growth in *Arabidopsis* response to phosphate deficiency. Plant J 94:315–326. https://doi.org/10.1111/tpj.13858

Swarup R, Kramer EM, Perry P, Knox K, Leyser HMO, Haseloff J, Beemster GTS, Bhalerao R, Bennett MJ (2005) Root gravitropism requires lateral root cap and epidermal cells for transport and response to a mobile auxin signal. Nat Cell Biol 7:1057–1065. https://doi.org/10.1038/ncb1316

Taniguchi YY, Taniguchi M, Tsuge T, Oka A, Aoyama T (2010) Involvement of *Arabidopsis thaliana* phospholipase Dζ2 in root hydrotropism through the suppression of root gravitropism. Planta 231:491–497. https://doi.org/10.1007/s00425-009-1052-x

Testerink C, Munnik T (2011) Molecular, cellular, and physiological responses to phosphatidic acid formation in plants. J Exp Bot 62:2349–2361. https://doi.org/10.1093/jxb/err079

Thompson CJ, Movva NR, Tizard R, Crameri R, Davies JE, Lauwereys M, Botterman J (1987) Characterization of the herbicide-resistance gene *bar* from *Streptomyces hygroscopicus*. EMBO J 6:2519–2523. https://doi.org/10.1002/j.1460-2075.1987.tb02538.x

Ueda T, Yamaguchi M, Uchimiya H, Nakano A (2001) Ara6, a plant-unique novel type Rab GTPase, functions in the endocytic pathway of *Arabidopsis thaliana*. EMBO J 20:4730–4741. https://doi.org/10.1093/emboj/20.17.4730

Uemura T (2016) Physiological roles of plant post-Golgi transport pathways in membrane trafficking. Plant Cell Physiol 57:2013–2019. https://doi.org/10.1093/pcp/pcw149

Uemura T, Ueda T, Ohniwa RL, Nakano A, Takeyasu K, Sato MH (2004) Systematic analysis of SNARE molecules in *Arabidopsis*: dissection of the post-Golgi network in plant cells. Cell Struct Funct 29:49–65. https://doi.org/10.1247/csf.29.49

Uemura T, Kim H, Saito C, Ebine K, Ueda T, Schulze-Lefert P, Nakano A (2012) Qa-SNAREs localized to the *trans*-Golgi network regulate multiple transport pathways and extracellular disease resistance in plants. Proc Natl Acad Sci USA 109:1784–1789. https://doi.org/10.1073/pnas.1115146109

Uemura T, Suda Y, Ueda T, Nakano A (2014) Dynamic behavior of the *trans*-Golgi network in root tissues of *Arabidopsis* revealed by super-resolution live imaging. Plant Cell Physiol 55:694–703. https://doi.org/10.1093/pcp/pcu010

Uemura T, Nakano RT, Takagi J, Wang Y, Kramer K, Finkemeier I, Nakagami H, Tsuda K, Ueda T, Schulze-Lefert P, Nakano K (2019) A Golgi-released subpopulation of the trans-Golgi network mediates protein secretion in *Arabidopsis*. Plant Physiol 179:519–532. https://doi.org/10.1104/pp.18.01228

Xing J, Li X, Wang X, Lv X, Wang L, Zhang L, Zhu Y, Shen Q, Baluška F, Šamaj J, Lin J (2019) Secretion of phospholipase Dδ functions as a regulatory mechanism in plant innate immunity. Plant Cell 31:3015–3032. https://doi.org/10.1105/tpc.19.00534

Yamaryo Y, Dubots E, Albrieux C, Baldan B, Block MA (2008) Phosphate availability affects the tonoplast localization of PLDζ2, an *Arabidopsis thaliana* phospholipase D. FEBS Lett 582:685–690. https://doi.org/10.1016/j.febslet.2008.01.039

Yao HY, Xue HW (2018) Phosphatidic acid plays key roles regulating plant development and stress responses. J Integr Plant Biol 60:851–863. https://doi.org/10.1111/jipb.12655

Yao H, Wang G, Guo L, Wang X (2013) Phosphatidic acid interacts with a MYB transcription factor and regulates its nuclear localization and function in *Arabidopsis*. Plant Cell 25:5030–5042. https://doi.org/10.1105/tpc.113.120162

Yoshimoto K, Hanaoka H, Sato S, Kato T, Tabata S, Noda T, Ohsumi Y (2004) Processing of ATG8s, ubiquitin-like proteins, and their deconjugation by ATG4s are essential for plant autophagy. Plant Cell 16:2967–2983. https://doi.org/10.1105/tpc.104.025395

Yu L, Nie J, Cao C, Jin Y, Yan M, Wang F, Liu J, Xiao Y, Liang Y, Zhang W (2010) Phosphatidic acid mediates salt stress response by regulation of MPK6 in *Arabidopsis thaliana*. New Phytol 188:762–773. https://doi.org/10.1111/j.1469-8137.2010.03422.x

Zhang W, Wang C, Qin C, Wood T, Olafsdottir G, Welti R, Wang X (2003) The oleate-stimulated phospholipase D, PLDδ, and phosphatidic acid decrease H_2O_2-induced cell death in Arabidopsis. Plant Cell 15:2285–2295. https://doi.org/10.1105/tpc.013961

Zhang W, Qin C, Zhao J, Wang X (2004) Phospholipase Dα1-derived phosphatidic acid interacts with ABI1 phosphatase 2C and regulates abscisic acid signaling. Proc Natl Acad Sci USA 101:9508–9513. https://doi.org/10.1073/pnas.0402112101

Zhang Y, Zhu H, Zhang Q, Li M, Yan M, Wang R, Wang L, Welti R, Zhang W, Wang X (2009) Phospholipase Dα1 and phosphatidic acid regulate NADPH oxidase activity and production of reactive oxygen species in ABA-mediated stomatal closure in *Arabidopsis*. Plant Cell 21:2357–2377. https://doi.org/10.1105/tpc.108.062992

Zhang Q, Lin F, Mao T, Nie J, Yan M, Yuan M, Zhang W (2012) Phosphatidic acid regulates microtubule organization by interacting with MAP65-1 in response to salt stress in *Arabidopsis*. Plant Cell 24:4555–4576. https://doi.org/10.1105/tpc.112.104182

Zhang B, Karnik R, Wang Y, Wallmeroth N, Blatt MR, Grefen C (2015) The Arabidopsis R-SNARE VAMP721 interacts with KAT1 and KC1 K^+ channels to moderate K^+ current at the plasma membrane. Plant Cell 27:1697–1717. https://doi.org/10.1105/tpc.15.00305

Zhang Q, Song P, Qu Y, Wang P, Jia Q, Guo L, Zhang C, Mao T, Yuan M, Wang X, Zhang W (2017) Phospholipase Dδ negatively regulates plant thermotolerance by destabilizing cortical microtubules in *Arabidopsis*. Plant Cell Environ 40:2220–2235. https://doi.org/10.1111/pce.13023

Zhang Q, Berkey R, Blakeslee JJ, Lin J, Ma X, King H, Liddle A, Guo L, Munnik T, Wang X, Xiao S (2018) Arabidopsis phospholipase Dα1 and Dδ oppositely modulate EDS1- and SA-independent basal resistance against adapted powdery mildew. J Exp Bot 69:3675–3688. https://doi.org/10.1093/jxb/ery146

Zhao J, Wang X (2004) *Arabidopsis* phospholipase Dα1 interacts with the heterotrimeric G-protein α-subunit through a motif analogous to the DRY motif in G-protein-coupled receptors. J Biol Chem 279:1794–1800. https://doi.org/10.1371/journal.pone.0028086

Zhao J, Wang C, Bedair M, Welti R, Sumner LW, Baxter I, Wang X (2011) Suppression of phospholipase Dγs confers increased aluminum resistance in *Arabidopsis thaliana*. PLoS ONE 6:e28086. https://doi.org/10.1371/journal.pone.0028086

Zhao J, Devaiah SP, Wang C, Li M, Welti R, Wang X (2013) Arabidopsis phospholipase Dβ1 modulates defense responses to bacterial and fungal pathogens. New Phytol 199:228–240. https://doi.org/10.1111/nph.12256

Zhukovsky MA, Filograna A, Luini A, Corda D, Valente C (2019) Phosphatidic acid in membrane rearrangements. FEBS Lett 593:2428–2451. https://doi.org/10.1002/1873-3468.13563

Zuo J, Niu QW, Chua N-H (2000) An estrogen receptor-based transactivator XVE mediates highly inducible gene expression in transgenic plants. Plant J 24:265–273. https://doi.org/10.1046/j.1365-313x.2000.00868.x